

\*Manuscript

[Click here to view linked References](#)

1  
2  
3  
4  
5  
6  
7  
8  
9  
10  
11  
12  
13  
14  
15  
16  
17  
18  
19  
20  
21  
22  
23  
24  
25  
26  
27  
28  
29  
30  
31  
32  
33  
34  
35  
36  
37  
38  
39  
40  
41  
42  
43  
44  
45  
46  
47  
48  
49  
50  
51  
52  
53  
54  
55  
56  
57  
58  
59  
60  
61  
62  
63  
64  
65

# Structural evolution of the Kopet Dagh fold-and-thrust belt (NE Iran) and interactions with the South Caspian Sea Basin and Amu Darya Basin

Alexandra M. M. Robert<sup>a,b</sup>, Jean Letouzey<sup>c</sup>, Mohammad A. Kavoozi<sup>d</sup>,  
Sharham Sherkati<sup>d</sup>, Carla Müller<sup>c</sup>, Jaume Vergés<sup>b</sup>, Abdollah Agababai<sup>d</sup>

<sup>a</sup>*Géosciences Environnement Toulouse (GET), Observatoire de Midi-Pyrénées,  
Université de Toulouse, CNRS, IRD, F-31400 Toulouse, France,  
(alexandra.robert@get.obs-mip.fr)*

<sup>b</sup>*Group of Dynamics of the Lithosphere (GDL), Institute of Earth Sciences Jaume  
Almera, ICTJA-CSIC, c Lluís Solé i Sabarís s/n, 08028 Barcelona, Spain*

<sup>c</sup>*Institut des Sciences de la Terre Paris (iSTeP), Sorbonne Universités, UPMC Univ  
Paris 06, UMR 7193, F-75005 Paris, France*

<sup>d</sup>*National Iranian Oil Company (NIOC), Exploration, Yaghma alley, Jomhuri ave,  
Tehran, Iran*

---

## Abstract

We present a detailed stratigraphic and structural study of the Kopet Dagh fold-and-thrust belt in NE Iran, which is an investigation of the complex polyphased tectonic history of this belt and its links with the adjacent South Caspian Sea and Amu Darya basins. Based on numerous field surveys, a large amount of 2D and 3D seismic data, borehole data and more than 150 new biostratigraphic datings, a new detailed biostratigraphic chart and 4 main regional cross-sections illustrate the importance of lateral facies variations and structural inheritance in the present-day structure of the belt.

After the Cimmerian orogeny corresponding to the closure of the Paleotethys Ocean in Late Triassic-Early Jurassic times, a post-collisional rifting event was associated with the deposition of one of the main source rocks of the Kopet Dagh and the Amu Darya Basin (Kashafrud Formation). Following

*Preprint submitted to Journal of Marine and Petroleum Geology*

*January 17, 2014*

1  
2  
3  
4  
5  
6  
7  
8  
9 this rifting event, over 7 km of sediments were accumulated until the Tertiary  
10 above a regional post-Triassic unconformity. The occurrence of local uplifts  
11 during the Late Cretaceous-Early Paleocene is interpreted as a consequence  
12 of regional-scale modification of plate-slab coupling in the Neotethys subduc-  
13 tion zone. The structures associated with the Late Eocene/Oligocene folding  
14 phase are sealed in the western part of the belt by a major Eocene-Oligocene  
15 unconformity at the base of the thick sedimentary series belonging to the  
16 South Caspian Sea Basin. The rapid subsidence of the South Caspian Sea  
17 Basin is probably related to syn-compressional downward flexure of the re-  
18 sistant basement basin at the onset of the Alpine phase. In the eastern part  
19 of the Kopet Dagh, this deformation is characterized by Middle Jurassic  
20 graben inversion with evidences of forced-folding, short-cuts and present-day  
21 slip partitioning, and as well by larger scale basement uplift. In contrast,  
22 the northwestern part of the belt shows thrust faults involving basement and  
23 fault-propagation folds within the sedimentary sequence. The Kopet Dagh  
24 presents an arcuate shape that follows the Paleotethys suture zone, which em-  
25 phasizes the importance of the structural inheritance and inversion processes  
26 in the present-day structures. Finally, a change from a mostly dip-slip to a  
27 mostly strike-slip tectonics occurred during the Pliocene within the Kopet  
28 Dagh as a consequence of a major tectonic reorganization in NE Iran.

29  
30  
31  
32  
33  
34  
35  
36  
37  
38  
39  
40  
41  
42  
43  
44  
45  
46  
47 *Keywords:* Kopet Dagh, Amu Darya Basin, South Caspian Sea Basin,  
48 Graben Inversion, Structural Geology, Seismic Sections  
49  
50

---

1  
2  
3  
4  
5  
6  
7  
8  
9  
10  
11  
12  
13  
14  
15  
16  
17  
18  
19  
20  
21  
22  
23  
24  
25  
26  
27  
28  
29  
30  
31  
32  
33  
34  
35  
36  
37  
38  
39  
40  
41  
42  
43  
44  
45  
46  
47  
48  
49  
50  
51  
52  
53  
54  
55  
56  
57  
58  
59  
60  
61  
62  
63  
64  
65

## 1. Introduction

2 Iran extended deformed zone is surrounded by the Turan Plate to the NE,  
3 which is part of stable Eurasia and by the Arabia Plate to the SW (Figure  
4 1a). Indeed, the Iranian geology is dominated by the long-standing conver-  
5 gence history between Eurasia and Gondwanan-derived terranes as indicated  
6 by numerous ophiolitic belts, fold-and-thrusts belts and resistant blocks that  
7 remain within the deformation zone. Two major compressional events, as  
8 a consequence of oceanic closures are described in Iran: (1) the Cimmerian  
9 orogeny, which is related to the closure of the Paleotethys Ocean and (2)  
10 the Alpine orogeny as a result of the closure of the Neotethys Ocean. In  
11 northeastern Iran, the Paleotethys Ocean separated the Turan Plate from  
12 Central Iranian blocks whereas the Neotethys Ocean opened on the southern  
13 margin of the Central Iranian blocks during the Permian (Muttoni et al.,  
14 2009) (Figure 1a). Besides, several ophiolitic domains (Nain Baft, Sabze-  
15 var, Sistan) cross-cut Central Iran and are interpreted as remnants of small  
16 oceanic domains that were closed during Paleocene to Eocene times (Agard  
17 et al., 2011).

18 In northeastern Iran, the Paleotethys suture zone corresponds to the bound-  
19 ary between the Kopet Dagh fold-and-thrust belt to the NE, and the east-  
20 ern prolongation of the Alborz range to the SW (Figure 1a). Remnants of  
21 the Paleotethys Ocean are located within the Binalud Mountains where the  
22 Cimmerian event is characterized by a collisional type event during the Late  
23 Triassic/Early Jurassic (Sheikholeslami and Kouhpeym, 2012). Following  
24 this collision, the Kopet Dagh Basin was deposited on the southern margin  
25 of the Turan Plate from the Jurassic to the Tertiary (Brunet et al., 2003).

1  
2  
3  
4  
5  
6  
7  
8  
9  
10 26 This basin was inverted during the Tertiary, because of the NE oriented con-  
11 27 vergence between Central Iran and Turan plates. Several authors studied  
12  
13 28 the metamorphism and the deformation associated with the closure of the  
14  
15 29 Paleotethys, but there are still few data on the structural and sedimentologic  
16  
17 30 evolution within the Kopet Dagh after the Cimmerian orogeny. Understand-  
18  
19 31 ing the evolution of the Kopet Dagh is important, because of its direct link  
20  
21 32 with the Amu Darya Basin to the NE and with the South Caspian Sea Basin  
22  
23 33 where lithological and structural information on Mesozoic rocks are rare, be-  
24  
25 34 cause of the important thickness of Tertiary sediments. The Amu Darya  
26  
27 35 Basin is a large basin that subsided during the Mesozoic after the closure of  
28  
29 36 the Paleotethys Ocean and which is located in Turkmenistan and Uzbekistan  
30  
31 37 extending southwestward into Iran and southeastward into Afghanistan (Ul-  
32  
33 38 mishek, 2004). This basin is a highly productive oil and gas province which  
34  
35 39 contains numerous giant gas fields such as Dauletabad, Yoloten, Shaltyk,  
36  
37 40 Bayram-Ali or Achak (see location on Figure 1b) (Ulmishek, 2004). Two  
38  
39 41 important gas fields are located to the East of the Kopet Dagh: the Khangir-  
40  
41 42 an and the Gonbadli, which produce from the Upper Jurassic carbonates  
42  
43 43 (Mozduran Formation) and the Lower Cretaceous siliciclastics (Shurijeh For-  
44  
45 44 mation) (Afshar-Harb, 1979; Aghanabati, 2004; Kavooosi et al., 2009a). These  
46  
47 45 two gas fields are located in anticlinal traps (Moussavi-Harami and Brenner,  
48  
49 46 1992) that include the 35 km-wide Khangiran anticline. The volume of re-  
50  
51 47 coverable gas reserves at Khangiran was estimated at 16.9 trillion cubic feet  
52  
53 48 by Iran Oil Ministry (2000) and the gas is piped from reneries to cities in  
54  
55 49 northeastern Iran. The main source rocks are considered to be the Middle  
56  
57 50 Jurassic shales and carbonates of the Chaman Bid Formation and the Upper



1  
2  
3  
4  
5  
6  
7  
8  
9  
10 51 Bajocian to Bathonian mudstones of the Kashafrud Formation.

11 52 In this article, we will focus on the structural evolution of Kopet Dagh fold-  
12  
13 53 and-thrust belt, with new stratigraphic and structural data, in order to set  
14  
15 54 up the sedimentologic and structural evolution of the belt since the closure  
16  
17 55 of the Paleotethys Ocean in Late Triassic/Lower Jurassic times. We will dis-  
18  
19 56 cuss the links between deformation in the Kopet Dagh and sedimentation in  
20  
21 57 the adjacent Amu Darya and South Caspian Sea basins, which constitute an  
22  
23 58 important contribution to unravel the structural evolution of the northern  
24  
25 59 Iranian region.

## 26 27 28 60 **2. Geological settings**

### 29 30 31 61 *2.1. Location and Morphology*

32  
33 62 This range marks the northern limit of the Alpine-Himalayan orogeny  
34  
35 63 in northeastern Iran and it also corresponds to the morphological boundary  
36  
37 64 between Turkmenistan and Iran which separates the Turan Plate, part of  
38  
39 65 stable Eurasia, from Central Iran over more than 600km (Figure 1a.).The  
40  
41 66 Kopet Dagh belt is an intra continental range which can be divided into  
42  
43 67 three different parts, (1) the northwestern part that is oriented N90, (2) the  
44  
45 68 northern part which mostly belongs to Turkmenistan and (3) the eastern part  
46  
47 69 which is N120 oriented (Figure 2). Different authors do not agree about the  
48  
49 70 extent of the Kopet Dagh belt and we will use the largest extent of the belt  
50  
51 71 and distinguish 3 main structural zones. The relief associated with the belt  
52  
53 72 dies out southeastwards towards Afghanistan, indicating the lack or small  
54  
55 73 amount of recent active tectonics in this part of the belt. The Kopet Dagh  
56  
57 74 range presents moderate elevations reaching 3120 m high in the southeastern

1  
2  
3  
4  
5  
6  
7  
8  
9  
10  
11  
12  
13  
14  
15  
16  
17  
18  
19  
20  
21  
22  
23  
24  
25  
26  
27  
28  
29  
30  
31  
32  
33  
34  
35  
36  
37  
38  
39  
40  
41  
42  
43  
44  
45  
46  
47  
48  
49  
50  
51  
52  
53  
54  
55  
56  
57  
58  
59  
60  
61  
62  
63  
64  
65

75 part of the belt to the North of Mashad city (Kuhha-ye Hezar Masjed sum-  
76 mit). The Main Kopet Dagh Fault marks the northeastern boundary of the  
77 belt and corresponds to a major inherited crustal-scale structure (Amurskiy,  
78 1971; Maggi et al., 2000). The presence of the Main Kopet Dagh Fault as a  
79 major crustal anisotropy is responsible of the localization of the deformation  
80 in the narrow Kopet Dagh fold-and-thrust belt (Lyberis and Manby, 1999).  
81 This 350 km-long fault delimits the southwestern boundary of the Kopet  
82 Dagh foredeep, part of the Amu Darya Basin deposited on the Turan Plate  
83 (Vernant et al., 2004) (Figure 1b). To the northwest, the Kopet Dagh belt is  
84 expressed as the Apsheron-Balkhan belt, delimiting the northern boundary  
85 of the South Caspian Sea Basin (Brunet et al., 2003) The southern bound-  
86 ary of the Kopet Dagh range is delimited by the Paleotethys suture zone  
87 marked by the Binalud Mountains (Wilmsen et al., 2009; Sheikholeslami and  
88 Kouhpeym, 2012) (Figure 1a.). To the SW of this suture zone, rocks are  
89 considered a prolongation of the Alborz fold-and-thrust belt (Alavi, 1992;  
90 Wilmsen et al., 2009).

## 91 *2.2. Geodynamical context*

92 North and Central Iran are located south of the Cimmerian belt, which  
93 marks the collision of the Iran Plate with the southern Eurasian margin  
94 (Sengor, 1990; Zanchi et al., 2006). The upper age limit of this collision is  
95 Late Triassic, as the Upper Triassic-Middle Jurassic Shemshak Group seals  
96 unconformably Cimmerian structures affecting the Paleozoic-Middle Triassic  
97 sequences of northern Alborz (Muttoni et al., 2009; Zanchi et al., 2006). The  
98 Kopet Dagh Basin was deposited after the Cimmerian orogeny (Garzanti and  
99 Gaetani, 2002) and more than 7 km of post-Triassic sediments were accumu-

1  
2  
3  
4  
5  
6  
7  
8  
9  
100 lated in this basin (Moussavi-Harami and Brenner, 1992). The onset of uplift  
101 within the Kopet Dagh is considered to have begun after 30Ma (Berberian  
102 and King, 1981; Golonka, 2004; Hollingsworth et al., 2010). From a geolog-  
103 ical point of view, (Lyberis and Manby, 1999) proposed that the inversion  
104 of the margin occurred during the Late Miocene as a response to the North-  
105 South convergence between Iran and Turan plates. However, post-Eocene  
106 sediments of the range are not well dated and more precise studies concern-  
107 ing the timing of inversion of the margin are needed. According to geodetic  
108 and geological data, between 4 and  $11\text{mm.yr}^{-1}$  of the present day northward  
109 Arabia-Eurasia convergence is accommodated in northeastern Iran (Vernant  
110 et al., 2004; Reilinger et al., 2006; Shabanian et al., 2009a, e.g.). The north-  
111 western strike of the convergence involves thrust faulting and minor left lat-  
112 eral strike-slip in the northwestern part of the belt and mainly right-lateral  
113 strike-slip faulting in the eastern part of the range (Figure 2). This observa-  
114 tion is confirmed by the earthquakes focal mechanisms that show thrusting  
115 to the West and strike-slip faulting with some thrusting to the east (Figure  
116 2). Furthermore, in the eastern part, recent strike-slip faulting across the  
117 belt is responsible of the dissection of the folds that can be observed to the  
118 East of Bojnurd city.

119  
120 According to geomorphologic data and datings, Shabanian et al. (2009b,  
121 2012) inferred that the important lateral motion recorded within the Kopet  
122 Dagh belt should not have started before the Early Pliocene ( $\sim 4$  Ma) which  
123 corresponds to the commonly proposed widespread reorganization of the tec-  
124 tonic deformation in the Arabia/Eurasia collision zone (Axen et al., 2001;

1  
2  
3  
4  
5  
6  
7  
8  
9  
10  
11  
12  
13  
14  
15  
16  
17  
18  
19  
20  
21  
22  
23  
24  
25  
26  
27  
28  
29  
30  
31  
32  
33  
34  
35  
36  
37  
38  
39  
40  
41  
42  
43  
44  
45  
46  
47  
48  
49  
50  
51  
52  
53  
54  
55  
56  
57  
58  
59  
60  
61  
62  
63  
64  
65

125 Allen et al., 2004; Copley and Jackson, 2006, e.g.). In contrast, Hollingsworth  
126 et al. (2008) propose that main strike-slip motion within the Kopet Dagh  
127 could have be initiated earlier, at  $\sim 10$  Ma, and that the initiation of this lat-  
128 eral motion could be related to the westward extrusion of the South Caspian  
129 Sea Basin relative to Central Iran and Eurasia.  
130 Nevertheless, especially in the eastern part of the belt, fold axes and strikes  
131 of the major tectonics features likely suggest a SW-NE oriented shortening,  
132 that probably reflects the tectonic settings before the reorganization of the  
133 tectonics deformation across the belt that we considered to have occurred at  
134  $\sim 4$ Ma as suggested by Shabanian et al. (2009b, 2012).

### 135 **3. Stratigraphic description**

136 We present our sedimentologic and biostratigraphic study that results  
137 from widespread and numerous field surveys performed by the NIOC team  
138 including 3 common field missions. Before this contribution, the stratigraphy  
139 in the Kopet Dagh was essentially based on facies recognition and correlation  
140 that resulted in differentiation of numerous formations, mainly according to  
141 lithological criteria. In this study, a widespread biostratigraphic study of the  
142 pelagic facies that have been correlated with precise lithological descriptions  
143 including more than 150 datings is presented, which allows us to propose  
144 a new stratigraphic chart for the Kopet Dagh and the surroundings basins  
145 (Figure 3). Our biostratigraphy is based on investigation of calcareous nanno-  
146 fossils. Age determination of the Mesozoic was performed from publications  
147 of Thierstein (1976) and Perch-Nielsen (1985) and we used the zonation given  
148 by Martini (1971) for the Cenozoic. Our results have been synthesized in the

1  
2  
3  
4  
5  
6  
7  
8  
9  
10 149 stratigraphic chart (Figure 3) and are also presented in Table 1 that indicates  
11 150 location of the main dated samples and names of the nannofossils.

12  
13 151 In this section, we will describe the detailed stratigraphy of the Kopet Dagh  
14 152 region, from the oldest outcropping rocks to the Tertiary continental sedi-  
15 153 ments.

16  
17  
18  
19 154 *3.1. Devonian to Upper Triassic: before the deposition of the Kopet Dagh*  
20 155 *Basin*

21  
22  
23 156 The oldest rocks outcropping in the Kopet Dagh fold-and-thrust belt are  
24 157 Devonian to Lower Carboniferous (Lyberis et al., 1998) and they are mostly  
25 158 outcropping within the Aghdarband erosional window, in the eastern part of  
26 159 the belt (Ruttner, 1991). Most of the sediments in this erosional window are  
27 160 Triassic in age and are strongly deformed as a consequence of the closure of  
28 161 the Paleotethys Ocean during the Cimmerian orogeny. Several unconformi-  
29 162 ties between the different series are observed.

30  
31 163 The Upper Devonian series are constituted at their base by dark grey thinly  
32 164 bedded volcanoclastics, shales and turbiditic sandstones. These series are  
33 165 overlain by dark green volcanoclastic sediments, with some limestone layers.  
34 166 The Lower Carboniferous is characterized by white limestones of about 200  
35 167 m thickness with the occurrence of some diabase dykes. The ?Late Permian  
36 168 to Lower Triassic molassic type rocks are composed of some red quartzitic  
37 169 sandstones and siltstones, with intercalated conglomerates that include peb-  
38 170 bles of quartz, pink colored granites, radiolarites and Carboniferous to Late  
39 171 Permian limestones. These series present a thickness up to 500 m.

40  
41 172 The Triassic series of the Aghdarband erosional windows can be distinguished  
42 173 in 4 main units: the three lowermost units that comprise an important

1  
2  
3  
4  
5  
6  
7  
8  
9  
10  
11  
12  
13  
14  
15  
16  
17  
18  
19  
20  
21  
22  
23  
24  
25  
26  
27  
28  
29  
30  
31  
32  
33  
34  
35  
36  
37  
38  
39  
40  
41  
42  
43  
44  
45  
46  
47  
48  
49  
50  
51  
52  
53  
54  
55  
56  
57  
58  
59  
60  
61  
62  
63  
64  
65

174 volcanic component were deposited before the Middle Cimmerian orogeny,  
175 whereas the fourth unit indicates deltaic conditions of deposition and results  
176 from the erosion of the relief formed during the Cimmerian orogeny (Rut-  
177 tner, 1991). In this study, we are not differentiating the different stages of  
178 the Cimmerian orogeny.

179 The Lower Triassic (T1) is characterized by red shales and sandstones with  
180 conglomerates including pebbles of quartz and red granites. Some tuffaceous  
181 shales are observed in the upper part, which are overlain by limestones dated  
182 as a Lower Triassic from the presence of ammonites. The Lower Triassic is  
183 also separated from the underlying sequence by a tectonic contact. The Mid-  
184 dle Triassic (T2) sequence starts with a conglomerate including only pebbles  
185 of the underlying limestone and is followed by volcanoclastic sandstone, and  
186 tuffaceous shales in the upper part. It is dated by two fossil horizons with  
187 abundant crinoids and ammonites, assigned to Landinian to Lower Carnian  
188 in age. The uppermost part of the Middle Triassic (T3) is marked by hard  
189 volcanoclastic sandstones and conglomerates. The Upper Triassic (T4) se-  
190 quence presents an unconformity at its base and starts with some sandstone  
191 without volcanic components and rich in coal layers on top of which there is  
192 some shale. These deposits, named the Miankuhi Formation, are dated by  
193 plant fragments as Upper Carnian and Lower Norian. The dark shales and  
194 ne-grained sandstones of the coal bearing Miankuhi Formation may represent  
195 an equivalent to the lower part of the Shemshak Group (Taheri et al., 2009;  
196 Wilmsen et al., 2009). Indeed, the lack of an equivalent to the widespread  
197 across the Iran Plate, Upper Triassic/Middle Jurassic Shemshak Group has  
198 been interpreted as a consequence of a period of emergence of the Turan

1  
2  
3  
4  
5  
6  
7  
8  
9  
10  
11  
12  
13  
14  
15  
16  
17  
18  
19  
20  
21  
22  
23  
24  
25  
26  
27  
28  
29  
30  
31  
32  
33  
34  
35  
36  
37  
38  
39  
40  
41  
42  
43  
44  
45  
46  
47  
48  
49  
50  
51  
52  
53  
54  
55  
56  
57  
58  
59  
60  
61  
62  
63  
64  
65

199 area (Lyberis et al., 1998). The Miankuhi Formation is intruded by coarse-  
200 crystalline leucogranites (Torbat-e-Jam Granite) that have been dated at 217  
201 +/- 1.7 Ma by (Zanchetta et al., 2013).

202 *3.2. Middle Jurassic: Sedimentation during the rifting following the Cimme-*  
203 *rian orogeny (Kashafrud Formation)*

204 Following the closure of the Paleotethys, the so-called Kopet Dagh Basin  
205 was deposited from the Middle Jurassic to the Tertiary and it corresponds  
206 to the southern border of the Amu Darya Basin. The sedimentation began  
207 with deposition of the Middle Jurassic Kashafrud Formation, which rests  
208 unconformably on folded Triassic or older rocks (Taheri et al., 2009). The  
209 Kashafrud Formation comprises 300 m to more than 2500 m of deep-marine  
210 siliciclastic strata (Poursoltani et al., 2007; Taheri et al., 2009). Furthermore,  
211 it could be either very thick, or absent above crest blocks or paleohighs. The  
212 Middle Jurassic Kashafrud Formation is generally conglomeratic at its base  
213 and consists of thick siltstones, sandstones and shales units. Where the whole  
214 formation is observed, the base presents more shaley facies and the top of the  
215 formation is characterized by shallower conditions of deposition as indicated  
216 by channelized sandstones typical of deltaic facies. Our biostratigraphic data  
217 indicate an Aalenian to Bajocian age for this formation (Figure 3 and Table  
218 1). This sequence was deposited in a rift system as indicated by the rapid  
219 facies and thickness variations (Kavoosi et al., 2009a). Some authors ar-  
220 gue a direct link during the deposition of the Kashafrud Formation between  
221 the Kopet Dagh Basin and the Neotethys Ocean (Poursoltani et al., 2007),  
222 whereas others proposed a rift basin model, which implies a direct relation-  
223 ship with the South Caspian Basin further West, rather than a link with the

1  
2  
3  
4  
5  
6  
7  
8  
9  
224 Neotethys Ocean (Taheri et al., 2009).

10  
11  
12 225 *3.3. Upper Jurassic (Chaman Bid and Mozduran Formations)*

13  
14 226 In the western part of the basin, the Kashafrud Formation is overlain  
15  
16 227 by the Upper Bajocian to Tithonian Chaman Bid Formation (Kalantari,  
17  
18 228 1969), which mostly consists of alternations of grey shales and marly lime-  
19  
20 229 stones. Main deposition environments of the Chaman Bid Formation are on  
21  
22 230 the slope of a carbonate platform and in the adjacent basin (Majadifard,  
23  
24 231 2003). In contrast, towards the East, the Kashafrud Formation is overlain  
25  
26 232 by the Upper Jurassic Mozduran Formation (Taheri et al., 2009), which is  
27  
28 233 the main gas reservoir in the Kopet Dagh range. The Mozduran Formation  
29  
30 234 is a well-bedded limestone in which several reefs systems have been observed  
31  
32 235 (Figure 4). Its facies varies towards the East to siliciclastic sediments. Fur-  
33  
34 236 thermore, the thickness of the Mozduran Formation varies from 200 m, to  
35  
36 237 800 m in the Khangiran gas eld and up to over 1400 m in the central part  
37  
38 238 of the belt (Afshar-Harb, 1979). The sharp and sudden lateral lithological  
39  
40 239 and thickness variations of the Mozduran Formation are interpreted as re-  
41  
42 240 lated to the presence of paleohighs within the basin after the Middle Jurassic  
43  
44 241 rifting in the Kopet Dagh Basin (Kavoosi et al., 2009b). The Mozduran  
45  
46 242 Formation is overlain by Cretaceous sediments, which are divided into 10  
47  
48 243 different formations (Shurijeh, Zard, Tirgan, Sarchashmeh, Sanganeh, Aita-  
49  
50 244 mir, Abderaz, Abtalkh, Neyzar and Kalat) and associated with a thickness  
51  
52 245 up to 4000 m thick in the western part of the basin (Afshar-Harb, 1979).  
53  
54 246 Emami et al. (2004) suggested that the late Cimmerian tectonic phase re-  
55  
56 247 sulted in widespread Late Jurassic-Early Cretaceous regression, leading to  
57  
58 248 deposition of the Lower Cretaceous continental siliciclastics and evaporites



1  
2  
3  
4  
5  
6  
7  
8  
9  
249 of the Shurijeh Formation.

10  
11  
12 250 *3.4. Lower Cretaceous, Neocomian (Shurijeh and Zard Formations)*

13  
14 251 The Lower Cretaceous Shurijeh Formation consists of red-bedded silici-  
15  
16 252 clastic sediments (sandstone, siltstone and conglomerates that are reservoir  
17  
18 253 rocks) overlain by limestones that present increasing thickness from the east-  
19  
20 254 ern part towards the central part of the belt. The upper part of the Lower  
21  
22 255 Cretaceous Shurijeh Formation consists of gypsum/anhydrite deposits that  
23  
24 256 were deposited in uvial to tidal at depositional settings under arid conditions  
25  
26 257 as a consequence of the major regression of the sea that occurred in the Juras-  
27  
28 258 sic/Cretaceous transition (Moussavi-Harami and Brenner, 1990; Moussavi-  
29  
30 259 Harami et al., 2009). These evaporite levels make the seal for the basal  
31  
32 260 Shurijeh Formation (secondary reservoir for gas in the Kopet Dagh range)  
33  
34 261 and the Mozduran Formations. The thickness of the Shurijeh Formation  
35  
36 262 ranges from 100 m above the paleohigh to about 1000 m thick (Afshar-Harb,  
37  
38 263 1979). Towards the NW, the Shurijeh Formation thickness decreases un-  
39  
40 264 til being completely replaced by the Zard Formation, which mainly consists  
41  
42 265 of marine marls, calcareous shale with some sandstone beds (Afshar-Harb,  
43  
44 266 1979). Our biostratigraphic results indicate a Berriasian age for this forma-  
45  
46 267 tion, but some outcrops indicate a minimum Late Kimmeridgian age (Jamali  
47  
48 268 et al., 2011), and a Tithonian age was assigned to the Shurijeh Formation  
49  
50 269 for its western most outcrops.  
51  
52  
53  
54  
55  
56  
57  
58  
59  
60  
61  
62  
63  
64  
65

1  
2  
3  
4  
5  
6  
7  
8  
9  
270 3.5. Lower Cretaceous, Aptian-Albian (Tirgan, Sarchashmeh and Sanganeh  
10  
11 271 Formations)

12  
13 272 The deposition of the continental Shurijeh Formation is followed by shal-  
14  
15 273 low marine sedimentation characterized by the deposition of the marls and  
16  
17 274 orbitolinids rich limestone Tirgan Formation with a thickness up to 600 m  
18  
19 275 to the West of the belt. The age of this series is Barremian and the nan-  
20  
21 276 nofossils are often strongly recrystallized and fragmented. The Sarchashmeh  
22  
23 277 Formation (about 150-250m thick) conformably overly the calcareous Tirgan  
24  
25 278 Formation and consists of two members: the lowest uniform grey marl unit  
26  
27 279 and the upper layer that consists of an alternance of shale and limestone. The  
28  
29 280 upper unit contains lumachelle layers deposited in at channels above which  
30  
31 281 about 1000 m thickness of marls were deposited. These thick marls become  
32  
33 282 richer in ne grained sandstone layers in the upper part which corresponds to  
34  
35 283 the dark grey shales of the Sanganeh Formation. From our biostratigraphic  
36  
37 284 study, a Late Barremian to Aptian age is proposed for the Sarchachmeh For-  
38  
39 285 mation and the Sanganeh Formation appears to be Albian in age. These  
40  
41 286 results disagree with Raisossadat and Shokri (2011) that proposed a Late  
42  
43 287 Barremian to Aptian for these 2 formations but we were able to date short  
44  
45 288 marine incursions as Late Albian in the Sanganeh Formation (Table 1).

46  
47 289 3.6. Upper Cretaceous (Aitamir, Abderaz, Abtalkh and Kalat Formations)

48  
49 290 The Aitamir Formation is a mudstone that grades upwards to a lower  
50  
51 291 glauconitic sandstone unit with cross-stratications, hummocky cross-stratications  
52  
53 292 and ripple marks, to a unit of mudstone intercalated with sandstone beds  
54  
55 293 (Sharafi et al., 2012). This formation corresponds to shallow open-marine  
56  
57 294 environment and its upper surface is delimited by a hiatus and local erosion

1  
2  
3  
4  
5  
6  
7  
8  
9  
10  
11  
12  
13  
14  
15  
16  
17  
18  
19  
20  
21  
22  
23  
24  
25  
26  
27  
28  
29  
30  
31  
32  
33  
34  
35  
36  
37  
38  
39  
40  
41  
42  
43  
44  
45  
46  
47  
48  
49  
50  
51  
52  
53  
54  
55  
56  
57  
58  
59  
60  
61  
62  
63  
64  
65

295 that is the first main hiatus in the Cretaceous sedimentation recorded in  
296 the Kopet Dagh range. This formation is barren of nannofossils which do  
297 not allow us to propose an age from biostratigraphy, but it is considered as  
298 Late Albian to Cenomanian (Sharafi et al., 2012). There is an important  
299 hiatus during the Turonian. Overlying this erosional surface, the Abderaz  
300 Formation is mostly made up of calcareous and marly shales (Allameh et al.,  
301 2010). Its thickness ranges between 200 and 400 m to the East of the Kopet  
302 Dagh and decreases towards the western part of the belt (Afshar-Harb, 1979).  
303 From our biostratigraphy study, a Late Santonian age was determined for the  
304 Abderaz Formation but the nannofossils are often strongly recrystallized and  
305 broken within the marl intercalations. According to a study based on ostra-  
306 cods, the sedimentation is considered to have taken place in a shallow open  
307 marine environment with warm climate conditions from the Late Turonian  
308 to the Early Santonian (Allameh et al., 2010).

309 The Abtalkh Formation is well developed in the eastern Kopet Dagh and  
310 has an almost uniform lithology consisting of calcareous shales with some  
311 lumachelle rich limestone beds near the top and with locally some small  
312 rudist-patch reefs. It presents a constant thickness of 700-800 m (Afshar-  
313 Harb, 1979). Our biostratigraphic study suggests Campanian ages for this  
314 formation. In the western part of the belt, the Abtalkh Formation is not  
315 developed and the Abderaz Formation is directly overlain by the Kalat For-  
316 mation. In contrast, to the East of the belt, the upper part of the Abtalkh  
317 Formation is characterized by a progressive transition to the Neyzar Forma-  
318 tion which is mostly composed of glauconite and clays with some sandstone  
319 in the upper levels indicating a shallow marine condition of sedimentation.

1  
2  
3  
4  
5  
6  
7  
8  
9  
10  
11  
12  
13  
14  
15  
16  
17  
18  
19  
20  
21  
22  
23  
24  
25  
26  
27  
28  
29  
30  
31  
32  
33  
34  
35  
36  
37  
38  
39  
40  
41  
42  
43  
44  
45  
46  
47  
48  
49  
50  
51  
52  
53  
54  
55  
56  
57  
58  
59  
60  
61  
62  
63  
64  
65

320 The transition between the Neyzar Formation to the Kalat transition is pro-  
321 gressive (Shahidi, 2008). The Kalat Formation is a widespread unit in the  
322 whole Kopet Dagh region and consists of a bioclastic limestone and carbon-  
323 ate buildups with subordinate sandstone beds observed only in the eastern  
324 part of the region (Afshar-Harb, 1979). This formation has been recently  
325 dated as Upper Campanian to Maastrichtian (Shahidi, 2008) and our bios-  
326 tratigraphic results indicate a Campanian age, but it was not possible to  
327 conrm the Maastrichtianage. The Kalat Formation consists of marls partly  
328 rich in gastropods and recifal limestones with rudists or algae, must have  
329 been deposited in a shallow shelf environment with a connection with the  
330 open sea (Afshar-Harb, 1979). The upper part of the Kalat Formation is  
331 marked by an erosional surface that is associated with the second general  
332 hiatus of sedimentation in the region.

333 *3.7. Paleogene (Pestehleigh, Chehel Kaman and Khangiran Formations)*

334 The transition between the Upper Campanian and the Paleocene is char-  
335 acterized by an increase of ne grained sandstones. The Paleocene Pestehleigh  
336 Formation is predominantly represented by red continental series with sand  
337 and siltstones with some conglomeratic levels at its base. It is followed by  
338 uviodeltaic and continental red sandstones and siltstones. Some marine in-  
339 cursions have been observed and dated within zone NP2 in the lowermost  
340 part and within zone NP5 upwards in the section. The uppermost Paleocene  
341 (zone NP9) was determined in the Chehel Kaman Formation that consists  
342 of white carbonates. The transition to the Lower Eocene is characterized  
343 by the occurrence of some layers of grey marls and red marls. The Eocene  
344 (zones NP12-NP19) is represented by alternating limestones and marls and

1  
2  
3  
4  
5  
6  
7  
8  
9  
10 345 it becomes sandier within the upper part.  
11

### 12 346 *3.8. Oligocene-Neogene*

13  
14 347 On geological maps, the youngest sediments represented are indicated as  
15  
16 348 Neogene in age. However, there is no published study about precise dating of  
17  
18 349 these continental series or neither about the deformation affecting these se-  
19  
20 350 ries. In this article, we decided to name this formation as Oligocene-Neogene  
21  
22 351 sediments. Most outcrops of the Oligocene-Neogene conglomerates and sand-  
23  
24 352 stones are represented as strongly discordant. Deposition of these sediments  
25  
26 353 is associated with the late reactivation of the fold belt.  
27

### 28 29 354 *3.9. Conclusions from the stratigraphic study*

30  
31 355 Our stratigraphic descriptions, synthesis and new biostratigraphic data  
32  
33 356 can be summarized as follows:

- 34  
35 357 1. There is a stratigraphic gap between the Lower Carboniferous and the  
36  
37 358 thick Permo-Triassic molassic type series that are in tectonic contact.  
38  
39 359 This unconformity might correspond to the Hercynian orogeny.  
40  
41 360 2. Some authors argue about several tectonic phases in the Cimmerian  
42  
43 361 orogeny (Eo-cimmerian and Middle Cimmerian orogenies), but because  
44  
45 362 this article is focused on the post-Cimmerian history, we will not dis-  
46  
47 363 tinguish these different phases and, instead, use the term of Cimmerian  
48  
49 364 orogeny.  
50  
51 365 3. The major unconformity observed within the range corresponds to the  
52  
53 366 base of the Kashafrud Formation (Middle Jurassic) which corresponds  
54  
55 367 to the first deposited sediments after the Cimmerian orogeny.  
56  
57  
58  
59  
60  
61  
62  
63  
64  
65

1  
2  
3  
4  
5  
6  
7  
8  
9  
10  
11  
12  
13  
14  
15  
16  
17  
18  
19  
20  
21  
22  
23  
24  
25  
26  
27  
28  
29  
30  
31  
32  
33  
34  
35  
36  
37  
38  
39  
40  
41  
42  
43  
44  
45  
46  
47  
48  
49  
50  
51  
52  
53  
54  
55  
56  
57  
58  
59  
60  
61  
62  
63  
64  
65

- 368 4. A rifting episode occurred in the Kopet Dagh region during the Middle  
369 Jurassic. At this time, the southern part of the Amu Darya Basin  
370 was probably linked with the South Caspian Sea Basin (Brunet et al.,  
371 2003). The abrupt facies and thickness changes of the Kopet Dagh  
372 Basin fill are inferred to mark activation of several major extensional  
373 faults during deposition of the Middle Jurassic Kashafrud Formation  
374 (Lyberis and Manby, 1999; Thomas et al., 1999).
- 375 5. During the Cretaceous and the Paleogene, several hiatus are interpreted  
376 as periods of emergence and the role of tectonics during these emergent  
377 periods could be questioned. These emergent periods are indicated as  
378 local uplifts in our stratigraphic chart (Figure 3). These hiatus have  
379 previously been interpreted a consequence of distal responses to colli-  
380 sional events (Berberian, 1983; Lyberis and Manby, 1999). However,  
381 there is no evidence of post-Middle Jurassic rifting as previously sug-  
382 gested by Lyberis and Manby (1999).
- 383 6. Finally, the late reactivation of the belt is not well dated, but occurred  
384 after the deposition of the marls of the Eocene Khangiran Formation.  
385 The occurrence of continental sedimentation is related to the struc-  
386 tural inversion that occurred after the Eocene as a consequence of the  
387 relative motion between the Iran Plate and the Turan Plate. This  
388 inversion resulted in widespread folding and thrusting of Jurassic to  
389 Tertiary sediments (Lyberis and Manby, 1999; Allen et al., 2003). This  
390 collision led to crustal shortening and right-lateral transpression which  
391 is still continuing as indicated by seismic activity (Thomas et al., 1999;  
392 Golonka, 2004) and active faulting (Hollingsworth et al., 2006, 2008,

1  
2  
3  
4  
5  
6  
7  
8  
9  
10  
11  
12  
13  
14  
15  
16  
17  
18  
19  
20  
21  
22  
23  
24  
25  
26  
27  
28  
29  
30  
31  
32  
33  
34  
35  
36  
37  
38  
39  
40  
41  
42  
43  
44  
45  
46  
47  
48  
49  
50  
51  
52  
53  
54  
55  
56  
57  
58  
59  
60  
61  
62  
63  
64  
65

393 2010; Shabanian et al., 2009a,b, 2012). Nevertheless, the margin inver-  
394 sion is not well dated, because of the lack of information of the precise  
395 timing of deposition of the post-Eocene sediments that are not widely  
396 outcropping in the range.

397 Our new stratigraphic results have been integrated in a detailed structural  
398 study of the belt focused on 4 main regional cross-sections. The next section  
399 presents the detailed and widespread structural study that we carried out  
400 across the Kopet Dagh range.

#### 401 **4. Geological cross-sections and structure of the Kopet Dagh range**

402 This part describes the main structures of the Kopet Dagh based on the  
403 simplified geological map (Figure 5) and on 4 regional cross-sections across  
404 the belt (Figures 6, 11, 13 and 15). These cross-sections result from numerous  
405 field surveys and our structural interpretation locally supported by 2D and  
406 3D seismic lines (see location of the presented seismic lines in Figure 5). Our  
407 field work was limited to the Iranian part of the range, which explains that  
408 the coverage of our data for the frontal part of the belt are restricted to  
409 seismic data (parts that connect with the South Caspian Sea region to the  
410 West and within the Amu Darya Basin to the NE). In the eastern part, the  
411 structural style of the front of the range has been dened using borehole data  
412 plus 2D and 3D seismic sections. Towards the South Caspian Sea Basin,  
413 folded structures are buried by the thick Oligocene to Quaternary sediments  
414 and numerous seismic lines are available in this transitional zone, above the  
415 Gorgan Plain. Two of our cross-sections (Figures 6 and 11) illustrate the  
416 links between the Kopet Dagh and the Amu Darya Basin, whereas the 2

1  
2  
3  
4  
5  
6  
7  
8  
9  
10  
11  
12  
13  
14  
15  
16  
17  
18  
19  
20  
21  
22  
23  
24  
25  
26  
27  
28  
29  
30  
31  
32  
33  
34  
35  
36  
37  
38  
39  
40  
41  
42  
43  
44  
45  
46  
47  
48  
49  
50  
51  
52  
53  
54  
55  
56  
57  
58  
59  
60  
61  
62  
63  
64  
65

417 others (Figures 13 and 15) are focused on the links between the Kopet Dagh  
418 and the South Caspian Sea Basin.

419 Pre-Cimmerian sediments outcrop in the Aghdarband erosional window  
420 and in some locations in the inner part of the belt. They have not yet been  
421 described in Afghanistan or in Turkmenistan. Then, there is only little and  
422 local information about the tectonic history before the Cimmerian orogeny  
423 within the Kopet Dagh. Furthermore, folds axes within the Upper Devonian  
424 to Lower Carboniferous strata are co-axial with the folds axes observed within  
425 Triassic rocks which causes difficulties to unravel tectonic effects resulting from  
426 the Hercynian orogeny than the one resulting from the Cimmerian orogeny.  
427 In this article, we will focus on the post-Cimmerian structural evolution of  
428 the fold-and-thrust belt. Following the Cimmerian orogeny, an extensional  
429 regime affected the southern Amu Darya Basin during the Middle Jurassic.  
430 From the Middle Jurassic to the Tertiary, over 7 km of sedimentary rocks  
431 were accumulated (Afshar-Harb, 1979) and they unconformably overlay Pa-  
432 leozoic and Triassic rocks (Ulmishek, 2004).

433 The thick sedimentary sequence is deformed as large-scale folds. The main  
434 crests of the Kopet Dagh range correspond to the fold axial regions of large  
435 anticlines mostly developed in the Lower Cretaceous limestones (Tirgan For-  
436 mation). In contrast, most of the valleys are located in the core of synclines  
437 occupied by less competent rocks. There is few Tertiary sediments outcrop-  
438 ping in the range, some of them are folded and outcrop in the center of large  
439 synclines, whereas some Oligocene-Neogene conglomerates are clearly discor-  
440 dant (Figure 5).

441 In the eastern part of the belt, the observed deformation is characterized



1  
2  
3  
4  
5  
6  
7  
8  
9  
10 442 by oblique Middle Jurassic graben inversion with evidences of forced-folding  
11 443 and few short-cuts, and as well by larger scale structures involving basement.  
12  
13 444 The large-scale structures present long axis those are parallel to the Main  
14  
15 445 Kopet Dagh Fault. From seismic sections, several dcollement levels within  
16  
17 446 the Mesozoic sequence explain numerous disharmonies, sh-tail structures in  
18  
19 447 the core of the folds or triangle zones (Figures 8 and 12). The orientation of  
20  
21 448 the Main Kopet Dagh Fault is interpreted as associated with the reactiva-  
22  
23 449 tion of old Paleozoic structures (Amurskiy, 1971; Maggi et al., 2000). Similar  
24  
25 450 striking Paleozoic structures are observed both within the Aghdarband Ero-  
26  
27 451 sional window (Zanchi et al., 2009; Zanchetta et al., 2013) and to the north-  
28  
29 452 eastern part of the Amu Darya Basin. Indeed, the Hercynian orogeny shaped  
30  
31 453 structural features trending roughly WNW-ESE inside the Turan Plate as  
32  
33 454 the Kyzylkum high, which marks the northeastern border of the Amu Darya  
34  
35 455 Basin. The orientation of the observed structures in the northern and eastern  
36  
37 456 part of the belt is directly related to the Alpine reactivation of these Paleozoic  
38  
39 457 basement structures. In contrast, in the northwestern part, the belt presents  
40  
41 458 an arcuate shape that follows the Paleotethys suture zone (Figure 1b). In  
42  
43 459 this part, the observed structures are thrust faults involving basement and  
44  
45 460 fault-propagation folds within the sedimentary sequence.

#### 461 *4.1. The eastern cross-section (Aghdarband-Gonbadly section)*

462 The eastern cross-section is a 140 km long NS geological cross-section  
463 extending from the Aghdarband erosional window to the wide anticline of  
464 the Khangiran gas eld (Figure 6, see location on Figure 5). This cross-  
465 section was created using our own field observations (Figure 7) and seismic  
466 lines including 3D seismic data and borehole data (Figures 8, 9 and 10). The

1  
2  
3  
4  
5  
6  
7  
8  
9  
10 467 Gonbadli and Khangiran gas fields are located in the Iranian part of the Amu  
11 468 Darya Basin and they extend to the Turkmen gas fields. This cross-section  
12  
13 469 will be described from the South to the North.  
14  
15

16 470 *4.1.1. To the South of the Aghdarband erosional window*  
17

18 471 The southern boundary of the cross-section corresponds to the prolonga-  
19  
20 472 tion of the Fariman Complex, interpreted as remnants of an intra-arc or incip-  
21  
22 473 ient back-arc basin (Zanchetta et al., 2013). The Middle Jurassic Kashafrud  
23  
24 474 Formation with evidences of syn-rift normal faulting outcrops to the North  
25  
26 475 of this ophiolitic complex. The occurrence of graben inversion and few short-  
27  
28 476 cuts within the Middle Jurassic Kashafrud Formation are highlighted in this  
29  
30 477 part of the cross-section. Towards the North, within the Kol Malek syncline,  
31  
32 478 Mesozoic sediments are thinner compared to the sediments belonging to the  
33  
34 479 Amu Darya Basin and they are conformably overlain by Cenozoic sediments.  
35  
36 480 The Kol Malek syncline is pinched and its northern ank is overthrust by  
37  
38 481 rocks belonging to the Darreh Anjir ophiolitic complex.  
39

40 482 *4.1.2. The Aghdarband erosional window*  
41

42 483 The basement of the South Amu Darya Basin is observed within the  
43  
44 484 Aghdarband erosional window. This basement consists of sedimentary, meta-  
45  
46 485 morphic and igneous rocks with ages ranging from Devonian to Triassic and  
47  
48 486 mostly corresponds to preserved fragments of a continental arc (Baud and  
49  
50 487 Stampfli, 1989; Poursoltani et al., 2007). The erosional window corresponds  
51  
52 488 to faulted and folded strata that are preserved below double verging thrusts  
53  
54 489 (Figure 7).  
55

56 490  
57  
58  
59  
60  
61  
62  
63  
64  
65

1  
2  
3  
4  
5  
6  
7  
8  
9  
10  
11  
12  
13  
14  
15  
16  
17  
18  
19  
20  
21  
22  
23  
24  
25  
26  
27  
28  
29  
30  
31  
32  
33  
34  
35  
36  
37  
38  
39  
40  
41  
42  
43  
44  
45  
46  
47  
48  
49  
50  
51  
52  
53  
54  
55  
56  
57  
58  
59  
60  
61  
62  
63  
64  
65

491 To the South of the window, the Darreh Anjir complex, consisting of gab-  
492 bros and low metamorphosed basalts, cherts and marbles (Zanchetta et al.,  
493 2013) is thrust on top of the northern flank of the Kol Malek syncline. The  
494 southern boundary of the complex is given by a south verging thrust which  
495 stacks the mostly mag rocks of the Darreh Anjir complex on the Late Triassic  
496 Miankuhi Formation, whereas, a thick succession of Upper Permian-Lower  
497 Triassic molassic-type sediments (conglomerates, sandstones and siltstones)  
498 overthrusts the northern boundary of the complex (Figure 7) (Zanchetta  
499 et al., 2013). Previous interpretations suggest that the Darreh Anjir com-  
500 plex corresponds to Paleotethys remnants (Ruttner, 1991; Alavi et al., 1997).  
501 However, a recent study suggests that this complex including both intrusive  
502 and lavas flows is, thus, remnants of a magmatic arc and related basins de-  
503 veloped on the southern Eurasia margin, to the NE of the Paleotethys suture  
504 zone (Zanchetta et al., 2013). The Paleozoic and Lower Mesozoic sediments  
505 deformed within the Aghdarband window derived from the erosion of the  
506 Hercynian orogen (Ruttner, 1991). The faults that are affecting these sedi-  
507 ments are laterally embedded by the Middle Jurassic Kashafrud Formation,  
508 which suggests a Cimmerian age for these faults.

509 Ruttner (1991) distinguished 4 members within the Triassic series: (T1)  
510 formed by limestones and conglomerates consisting of limestones pebbles,  
511 overlain by alternance of tuffaceous sandstone and limestone beds, (T2) con-  
512 sisting of tuff and tuffaceous sandstones with a basal conglomerate contain-  
513 ing quartz pebbles, (T3) made of tuaceous sandstone, so-called tuff and some  
514 shales at its top and (T3a), the Miankuhi Formation which is marked by a  
515 coal horizon at its base overlain by sandstone layers. The T1, T2 and T3

1  
2  
3  
4  
5  
6  
7  
8  
9  
10 516 series are characterized by an important volcanic input suggesting that they  
11 517 derived from the erosion of a volcanic arc. To the North, the low metamor-  
12  
13 518 phosed molassic succession overthrusts Triassic units that are forming a large  
14  
15 519 south-verging syncline marked in its central part by a narrow anticline and  
16  
17 520 some coal-rich sediments of the Miankuhi Formation outcrop in the core of  
18  
19 521 the syncline. The northern flank of the large syncline is bounded by an-  
20  
21 522 other double-verging syncline presenting secondary order folds in its core.  
22  
23 523 Its northern boundary is marked by several narrow strips of steeply inclined  
24  
25 524 Triassic rocks that are interpreted as due to a flower structure. Indeed, to-  
26  
27 525 wards the North, a steep vertical Cimmerian fault striking WNW-ESE with  
28  
29 526 dextral strike-slip component has been described and separates the slightly  
30  
31 527 deformed Triassic sediments from the more deformed Devonian and Carbonif-  
32  
33 528 erous sediments (Zanchi et al., 2010). Devonian sediments consist of folded  
34  
35 529 turbiditic series, whereas, the Carboniferous strata are white marbles with  
36  
37 530 diabase intrusions. The fold axes observed in Devonian and Carboniferous  
38  
39 531 sediments are coaxial with the ones observed within the Triassic, which does  
40  
41 532 not allow easily distinguishing the deformation associated with the Cimme-  
42  
43 533 rian orogeny from the one associated with the Hercynian orogeny. To the  
44  
45 534 North of the Aghdarband erosional window, the Middle Jurassic Kashafrud  
46  
47 535 Formation overlay unconformably the Devonian strata.

48  
49 536 *4.1.3. To the North of the Aghdarband window*

50  
51 537 To the North of the Aghdarband window, seismic data suggest a triangle  
52  
53 538 (or fish-tail) structure (Figure 8). The older than the Late Cretaceous (Cam-  
54  
55 539 panian) series are force-folded and thrust to the NE, whereas, the younger  
56  
57 540 series (uppermost Cretaceous and Tertiary) form a wide monocline towards

1  
2  
3  
4  
5  
6  
7  
8  
9  
10 541 the NE. This is interpreted as a consequence of a triangle zone associated  
11 542 with disharmony and back-shearing within Late Cretaceous marls. During  
12  
13 543 our field missions, we also observed some thrusting to the SW due to minor  
14  
15 544 dcollements within the Middle or Upper Jurassic shales.  
16  
17 545 Towards the NE, the Mesozoic and Cenozoic series of the South Amu Darya  
18  
19 546 Basin are imaged on the 2D and 3D seismic lines available in the Gonbadli  
20  
21 547 and Khangiran gas elds area (Figures 9 and 10). Late Jurassic to Late Eocene  
22  
23 548 series slightly thick away from the Aghdarband erosional window, which sug-  
24  
25 549 gests that the region formed a persistent paleorelief during the deposition of  
26  
27 550 the South Amu Darya Basin.  
28  
29 551 The seismic sections (Figure 9) supported with field evidences indicate that  
30  
31 552 the Middle Jurassic Kashafrud Formation was deposited in a rift system,  
32  
33 553 which is consistent with the occurrence of conglomeratic levels at the base of  
34  
35 554 the formation covered by clastic deposits. Furthermore, there are important  
36  
37 555 lateral variations in thickness of the Kashafrud Formation from no deposi-  
38  
39 556 tion on the crests of the blocks to several kilometers thick in the hanging  
40  
41 557 wall of the normal faults. Forced folding as a consequence of the inversion  
42  
43 558 of a major Middle Jurassic rift faults system is observed on seismic sections  
44  
45 559 (Figure 10). Some Tertiary en echelon faults can be observed on the 3D  
46  
47 560 seismic block on the top of the basement uplift shown in Figure 9a, indicat-  
48  
49 561 ing a dextral component during the Tertiary inversion along the WNW-ESE  
50  
51 562 trending structures.  
52  
53 563 Some carbonate build-up and progradations within the Upper Jurassic car-  
54  
55 564 bonatic sequence are observed (indicated by the black arrow in Figure 10  
56  
57 565 similar to the ones we observed in the field (Figure 4b).  
58  
59  
60  
61  
62  
63  
64  
65

1  
2  
3  
4  
5  
6  
7  
8  
9  
10 566 *4.1.4. Summary of the Aghdarband-Gonbadly cross-section*

11 567 The Aghdarband-Gonbadly cross-section shows a major basement inver-  
12  
13 568 sion that affects the southern border of the Amu Darya Basin. A progressive  
14  
15 569 thinning of the Jurassic and Cretaceous series of the basin towards the NE, as  
16  
17 570 well as the occurrence of more pelagic facies to the North and more continen-  
18  
19 571 tal facies towards the Aghdarband erosional window, suggest that the region  
20  
21 572 of the erosional window formed a persistent paleorelief during the deposi-  
22  
23 573 tion of the series of the basin. Deposition of the Middle Jurassic Kashafrud  
24  
25 574 Formation occurred during active rifting as highlighted by numerous normal  
26  
27 575 offsets shifting the base of this formation. Locally, the rift system has been  
28  
29 576 inverted as suggested by the observation of forced-folding within the Upper  
30  
31 577 series, which is attributed to the Tertiary inversion of the range. This late  
32  
33 578 tectonic inversion is associated with an important strike-slip component, and  
34  
35 579 with the development of growth strata within the Tertiary sediments. There  
36  
37 580 is little information in the Turkmen part of this cross-section but several gas  
38  
39 581 fields are producing from the clastic series of the Early Cretaceous Shuri-  
40  
41 582 jeh Formation or from the reefal carbonates of the Late Jurassic Mozduran  
42  
43 583 Formation capped by the Late Jurassic-Early Cretaceous evaporites and salt  
44  
45 584 layers within the Amu Darya Basin.

46  
47 585 *4.2. Darre Gaz cross-section*

48  
49 586 The 160 km-long DarreGaz cross-section is passing through the Darre Gaz  
50  
51 587 syncline where the Tertiary series are the thickest observed within the range  
52  
53 588 (Figure 11). This cross-section highlights the front of the Kopet Dagh and it  
54  
55 589 is passing through the area where there are numerous recent strike-slip faults  
56  
57 590 that cross-cut the structures. Along this cross-section, the sedimentary series

1  
2  
3  
4  
5  
6  
7  
8  
9  
10  
11  
12  
13  
14  
15  
16  
17  
18  
19  
20  
21  
22  
23  
24  
25  
26  
27  
28  
29  
30  
31  
32  
33  
34  
35  
36  
37  
38  
39  
40  
41  
42  
43  
44  
45  
46  
47  
48  
49  
50  
51  
52  
53  
54  
55  
56  
57  
58  
59  
60  
61  
62  
63  
64  
65

591 are thicker than along the Aghdarband-Gonbadly cross-section and presents  
592 uplifted deeper facies. For this cross-section, seismic sections only exist in the  
593 Darre Gaz region. Thicknesses of the formations were estimated according to  
594 field observations, seismic data and satellite imaging, because of the lack of  
595 borehole data. As for the eastern cross-section, the basement is also implied  
596 in the deformation and several dcollement levels within the Mesozoic series  
597 are observed. This cross-section will be described from the SW to the NE.

598 *4.2.1. Description of the Darre Gaz cross-section*

599 In the southwestern part of the cross-section, the folded structures present  
600 a wavelength of about 12 km and they are cut by several strike-slip faults.  
601 We infer that the folding of the series could be associated with the inversion  
602 of Middle Jurassic grabens. The strike-slip faults affect the discordant Ter-  
603 tiary series and are associated with the most recent tectonics affecting this  
604 belt.

605 The seismic section shown in Figure 12 is located along the structural section.  
606 It highlights an important disharmony between deep and surface structures,  
607 with several dcollements levels within the thick Cretaceous series. Main  
608 dcollement levels are located within the Kashafrud Formation, within the  
609 evaporitic levels of the Suriyeh Formation and within the thick marly Sar-  
610 chashmeh and Sanganeh formations. Some structures are outcropping lat-  
611 erally, such as the narrow reverse fold affecting the Barremian limestones  
612 of the Tirgan Formation. Finally, the northeastern part of the cross-section  
613 corresponds to the Zarrineh Kuh anticline that forms the front of the Kopet  
614 Dagh range. Seismic data (Figure 12) show 2 anticlines: (1) the shallower  
615 anticline that affects Cretaceous and Paleocene levels and that is narrower

1  
2  
3  
4  
5  
6  
7  
8  
9  
10  
11  
12  
13  
14  
15  
16  
17  
18  
19  
20  
21  
22  
23  
24  
25  
26  
27  
28  
29  
30  
31  
32  
33  
34  
35  
36  
37  
38  
39  
40  
41  
42  
43  
44  
45  
46  
47  
48  
49  
50  
51  
52  
53  
54  
55  
56  
57  
58  
59  
60  
61  
62  
63  
64  
65

616 than (2) the deeper one, in which the Jurassic series are affected by larger  
617 wavelength forced-folding. There are no seismic data along the section cross-  
618 ing the Zarrineh Kuh anticline but, seismic profiles of its southwestern flank  
619 highlight the important disharmony between shallow and deep structures.

#### 620 *4.2.2. Summary of the Darre Gaz cross-section*

621 The Darre Gaz cross-section highlights the importance of forced-folding  
622 affecting the basement and overlain by shorter wavelength folds detached  
623 along several decollement levels. Surrounding seismic sections show that the  
624 dcollement level of the frontal fold is located within the Lower Cretaceous,  
625 probably within the evaporitic levels. This cross-section attests of the im-  
626 portant partitioning of the recent deformation across the belt: thrusts are  
627 located in the frontal part of the range as highlighted by compressional fo-  
628 cal mechanisms whereas mostly strike-slip deformation is now affecting the  
629 internal parts of the range.

#### 630 *4.3. Western Kopet Dagh cross-section*

631 This 90 km-long regional cross-section (Figure 13) cuts across the west-  
632 ern branch of the Kopet Dagh range, from the internal zone until the South  
633 Caspian Sea Basin. It is a dog-leg type cross-section based on available out-  
634 crops and it presents typical structures and unconformities characterizing  
635 this area. Thickness variations have been observed on the field. At large  
636 scale, this section shows the uplift and erosion of the inner part of the Kopet  
637 Dagh as a consequence of several periods of uplift and/or folding. The south-  
638 western part of this section corresponds to the inner part of the belt, where  
639 several basement thrusts are observed and where Paleozoic and Mesozoic for-



1  
2  
3  
4  
5  
6  
7  
8  
9  
10 640 mations outcrops at several locations. In this area, the folds of the western  
11 641 part of the Kopet Dagh are oriented SW-NE (Figure 5) and plunge to the  
12  
13 642 SW in the Gorgan Plain below the sediments of the South Caspian Sea Basin.  
14

15  
16 643 *4.3.1. Description of the western Kopet Dagh cross-section*  
17

18 644 We will describe this cross-section from the internal zone, close to the  
19  
20 645 Late Triassic/Early Jurassic Paleotethys suture zone towards the Gorgan  
21  
22 646 Plain corresponding to the eastern prolongation of the South Caspian Sea  
23  
24 647 Basin. The large wavelength structures present a SE vergence until Balkor  
25  
26 648 syncline (Figure 13). In contrast, the structures that plunge beneath the  
27  
28 649 Gorgan Plain present an opposite NW vergence.

29  
30 650 The southeastern part of the cross-section corresponds to a large SE-verging  
31  
32 651 anticline (Figure 13) formed by the series from Paleozoic to Eocene in age.  
33  
34 652 On top of the Paleozoic, Triassic series (shales, grey-yellow dolomites and  
35  
36 653 basalts) are outcropping and unconformably overlain by a conglomeratic level  
37  
38 654 corresponding to the base of the Middle Jurassic Kashafud Formation. The  
39  
40 655 Kashafud Formation presents a fan geometry and its thickness is locally up  
41  
42 656 to 2500 m in the deeper parts of this rift structure (Figure 14).

43 657 The Middle Jurassic Kashafud Formation overlays lower series (Paleozoic  
44  
45 658 or Triassic series) and is unconformably covered by the marls of the Upper  
46  
47 659 Jurassic Chaman Bid Formation that could locally directly overly the Trias-  
48  
49 660 sic strata. This erosion on top of the Kashafud Formation was also observed  
50  
51 661 on some seismic lines in the eastern part of the Kopet Dagh (Kavoosi et al.,  
52  
53 662 2009b). Above a thin marly and clastic level, the Lower Cretaceous Tirgan  
54  
55 663 limestone reaches around 450 m of thickness. On the top of the Tirgan For-  
56  
57 664 mation, there are numerous sedimentation lacunas and it is locally covered  
58  
59  
60  
61  
62  
63  
64  
65

1  
2  
3  
4  
5  
6  
7  
8  
9  
10 665 by the very thin Sarchashmeh Formation or by the Abderaz Formation. The  
11 666 whole Upper Cretaceous series do not reach 400 m of thickness and they  
12  
13 667 are overlain by the reddish series of the Paleocene. There is an important  
14  
15 668 thinning of the Mesozoic series and in particular of the Lower Cretaceous  
16  
17 669 with an important lacuna of deposition from the Aptian to the Turonian that  
18  
19 670 has only been observed in the western Kopet Dagh. Large out-of-sequence  
20  
21 671 thrusts that affect the whole stratigraphic sequence are observed (Figure 14).  
22  
23 672 They are obliquely cutting the previous structures such as the Kashafrud  
24  
25 673 rift, which suggests that they are newly-formed and do not correspond to  
26  
27 674 inversion of the rift faults. Limestones of the Tirgan Formation are folded  
28  
29 675 and faulted with a short wavelength which suggests the occurrence of local  
30  
31 676 decollement levels within the underlying Chaman Bid Formation. The series  
32  
33 677 is continuing towards the West (Figure 14) with the occurrence of folds with  
34  
35 678 Kashafrud and Mozduran formations in the core that are cross-cut by the  
36  
37 679 newly-formed South-verging thrusts. To the North, within the northern flank  
38  
39 680 of the Bash Kalateh anticline, the Lower Cretaceous series (1300 m thick) are  
40  
41 681 outcropping, whereas they were absent in the Nabiya syncline. They consist  
42  
43 682 of calcareous with clastic components of the Zard Formation and expand up  
44  
45 683 to the Aitamir Formation characterized by its limonitic shales.  
46  
47 684 Conglomerates (~40 m thick) are characterized an erosion level on the top  
48  
49 685 of the Aitamir Formation and they are overlain by the white limestones of  
50  
51 686 the Abderaz Formation that are the only sediments from the Upper Creta-  
52  
53 687 ceous. The marine marls of the Eocene directly overlie the Upper Cretaceous.  
54  
55 688 The entire series is concordant and presents a constant dipping whereas the  
56  
57 689 Oligocene-Neogene conglomerate is subhorizontal. Toward the NW, a nar-

1  
2  
3  
4  
5  
6  
7  
8  
9  
10 690 row South-verging anticline with a core made of Upper Jurassic Mozduran  
11 691 Formation is thrust to the South by the Takal Kuh Fault. The Lower  
12 692 Cretaceous series thickens and is unconformably overlain by sediments from  
13 693 the Upper Cretaceous Kalat Formation to the Eocene Khangiran Formation.  
14 694 NW verging large anticlines and synclines are observed, as well as an im-  
15 695 portant thickening of the Lower Cretaceous series that is related to a higher  
16 696 initial thickness and to the occurrence of thrusting within this formation. In  
17 697 contrast, there is a lack of most of the Upper Cretaceous in the last syncline  
18 698 (Rud Atkak syncline) that has a core made of Paleocene sediments. At the  
19 699 western end of the section, some seismic lines illustrate that the folds of the  
20 700 Kopet Dagh are plunging laterally below the Gorgan plain sediments (Fig-  
21 701 ure refloca). Along the section, an important angular unconformity between  
22 702 the folded Aitamir Formation and the Oligocene-Neogene conglomerates is  
23 703 observed. We have already observed the folded Eocene sediments that have  
24 704 been eroded before the deposition of a sub-horizontal Oligocene-Neogene con-  
25 705 glomerate. The seismic sections show buried anticlines and the post-Eocene  
26 706 unconformity, which is affected by some recent thrust faults. A drill was  
27 707 done in this region, but due to numerous thrusts and repetitions, it did not  
28 708 reach the Lower Cretaceous Tirgan carbonates.

29  
30  
31  
32  
33  
34  
35  
36  
37  
38  
39  
40  
41  
42  
43  
44  
45  
46 709 *4.3.2. Summary of the western Kopet Dagh cross-section*

47  
48 710 This cross-section is characterized by important lateral variations of the  
49 711 formations thicknesses as a consequence of either several unconformity or  
50 712 lateral sediment thickness variations inherited from the deposition of the  
51 713 series. There is a lacuna in the Lower Cretaceous to the East and in the  
52 714 Upper Cretaceous to the West. There are also facies variations and thick-

1  
2  
3  
4  
5  
6  
7  
8  
9  
10  
11  
12  
13  
14  
15  
16  
17  
18  
19  
20  
21  
22  
23  
24  
25  
26  
27  
28  
29  
30  
31  
32  
33  
34  
35  
36  
37  
38  
39  
40  
41  
42  
43  
44  
45  
46  
47  
48  
49  
50  
51  
52  
53  
54  
55  
56  
57  
58  
59  
60  
61  
62  
63  
64  
65

715 ening of the Lower Cretaceous toward the West. The unconformity at the  
716 base of the Lower Cretaceous (Kalat Formation) is truncated by the post-  
717 Eocene unconformity. These several erosional surfaces are associated with  
718 stratigraphic lacunas are observed from the Lower Cretaceous to the Eocene,  
719 but they are not associated with angular unconformities, in contrast to the  
720 major angular unconformity characterizing the base of the post-Eocene se-  
721 ries. The entire series until the Late Eocene is folded within double-verging  
722 structures. Newly-formed thrusts cross-cut the previous structures of the  
723 Kashafrud graben.

724 *4.4. Gorgan Plain cross-section: from the Eastern Caspian Sea margin to*  
725 *the Gorgan Plain*

726 This part presents the westernmost Kopet Dagh cross-section that is  
727 linked with the eastern part of the South Caspian Sea Basin above the Gor-  
728 gan Plain (Figure 15). The Gorgan Plain is the southern prolongation of a  
729 larger delta that outcrops in Turkmenistan, along the Caspian Sea. Numer-  
730 ous wells and discoveries were made in this region where the fields present an  
731 arcuate shape along the coast (Figure 1b) and produce into the Lower and  
732 Middle Pliocene clastic series. In this region, the folds are oriented SWS-  
733 ENE, but they are masked by the Quaternary sediments that outcrop in the  
734 Gorgan Plain in Iran. Discovery of gas and condensates was made in one of  
735 this buried folded structure, within the Lower Cretaceous carbonates of the  
736 Tirgan Formation.

1  
2  
3  
4  
5  
6  
7  
8  
9 737 *4.4.1. Description of the Gorgan Plain cross-section*

10  
11 738 According to borehole data and similarly to the western Kopet Dagh  
12  
13 739 cross-section, the Gorgan Plain cross-section shows an important angular  
14  
15 740 unconformity between folded and transgressive series that are consequent to  
16  
17 741 the important Tertiary subsidence in the South Caspian Sea Basin. The folds  
18  
19 742 affecting the Upper Cretaceous series present an asymmetry towards the NW  
20  
21 743 and they prolong the folded structures belonging to the Kopet Dagh range  
22  
23 744 (Figure 15) as attested by borehole data and seismic sections (Figures 16 and  
24  
25 745 17).

26 746 Above the unconformity, progressive onlap of the series characterizes the  
27  
28 747 border of the South Caspian Sea Basin. However, these series as well as the  
29  
30 748 unconformity are locally slightly folded as a consequence of the late Alpine  
31  
32 749 phase.

33  
34 750 Figure 17 presents a composite seismic section close to the Caspian Sea coast  
35  
36 751 and shows the prolongation of the folded structures underneath the uncon-  
37  
38 752 formity, which is affected by local reactivation. Above the unconformity, the  
39  
40 753 clastic series thickens greatly towards the South Caspian Sea as a consequence  
41  
42 754 of several transgressive episodes. Regional correlations enable to propose that  
43  
44 755 the yellow horizon nearly corresponds to the top-Miocene. Between the yellow  
45  
46 756 horizon and the unconformity, normal faults sitted on top of a disharmony  
47  
48 757 are observed, highlighting a shale ridge structure (indicated with the (M?)  
49  
50 758 on the Figure 17). The clay series of the Oligocene Maykop Formation of the  
51  
52 759 South Caspian Sea Basin are often responsible of the development of shale  
53  
54 760 ridges type structures, which suggests an Oligocene age for the series sitting  
55  
56 761 on top of the unconformity.

1  
2  
3  
4  
5  
6  
7  
8  
9  
10  
11  
12  
13  
14  
15  
16  
17  
18  
19  
20  
21  
22  
23  
24  
25  
26  
27  
28  
29  
30  
31  
32  
33  
34  
35  
36  
37  
38  
39  
40  
41  
42  
43  
44  
45  
46  
47  
48  
49  
50  
51  
52  
53  
54  
55  
56  
57  
58  
59  
60  
61  
62  
63  
64  
65

762 *4.4.2. Summary of the Gorgan Plain cross-section*

763 This cross-section shows the relationship between the Kopet Dagh anity  
764 folds uplifted and eroded after the Eocene marine transgression. The trend  
765 of the buried folds is SSW-NNW, which is parallel to the structures of the  
766 western part of the Kopet Dagh range. The processes involved for the onset  
767 of the rapid Oligocene until recent times subsidence is still debated but sev-  
768 eral authors proposed a syn-compressional downward buckling of the basin  
769 resistant basement (Korotaev et al., 1999) and/or the onset of the subduc-  
770 tion below the Apsheron ridge (Allen et al., 2003). Progressive onlap above  
771 the unconformity in the Gorgan Plain are observed within the Oligo-Miocene  
772 clastic sediments. The trend of the Maykop ridge along the coast of the Turk-  
773 menistan suggests an Oligo-Miocene paleodelta of the Amu Darya river in  
774 that region. This proto-delta shifts to the N during the Pliocene, possibly as  
775 a consequence to the rapid uplift within the Kopet Dagh and Alborz ranges  
776 at that time.

777 **5. Discussions on the geodynamic evolution**

778 Based on our new stratigraphic and structural data correlated with al-  
779 ready published data, we decipher the geodynamic evolution of the Kopet  
780 Dagh range and its relationships with the adjacent Amu Darya and South  
781 Caspian Sea basins (Figures 18 and 19).

782 *5.1. Late Triassic to Early Jurassic*

783 The collision between Central Iran and Turan plates (Cimmerian orogeny)  
784 follows the northward subduction of the Paleotethys Ocean and occurred

1  
2  
3  
4  
5  
6  
7  
8  
9 785 during the latest Triassic/Early Jurassic (Zanchetta et al., 2013) (Figure  
10 786 18a). The trend of the main structures of the northwestern and eastern parts  
11 787 of the Kopet Dagh follows the arcuate shape of the Paleotethys suture zone,  
12 788 which emphasizes the importance of the structural inheritance in the present-  
13 789 day structure of the belt. Furthermore, some authors suggest an important  
14 790 oblique component of the convergence from a detailed structural study on  
15 791 transpressional structures within the Aghdarband window (Zanchi et al.,  
16 792 2010). They infer the reactivation of some Paleozoic structures as major  
17 793 strike-slip faults during the Cimmerian orogeny. Those linear structures are  
18 794 observed North of the Amu Darya Basin (Mangyshlak and Ustyurt ridges)  
19 795 and within the Kopet Dagh (Main Kopet Dagh Fault) and they have been  
20 796 recently reactivated too (Ulmishek, 2001). From a petroleum point of view,  
21 797 the coal beds of the Upper Triassic sequence (Miankuhi Formation) could be  
22 798 a potential source rock but this formation was deposited within the narrow  
23 799 Aghdarband back-arc basin (Zanchetta et al., 2013) and it is hard to infer  
24 800 its present extension.

## 41 801 *5.2. Middle Jurassic*

42 802 After the Cimmerian collision (Figure 18b), a post-orogenic rifting phase  
43 803 took place across the studied area with the deposition of the clastic Middle  
44 804 Jurassic Kashafrud Formation. Seismic sections show that the Middle Juras-  
45 805 sic Kashafrud Formation was deposited in a rift system, as suggested by the  
46 806 lack or near lack of this formation above pre-Jurassic basement highs in op-  
47 807 position within the hanging wall of the normal faults where this formation  
48 808 reaches several thousand meters thick. Furthermore, evidences of preserved  
49 809 Middle Jurassic normal faulting have been observed at several places in the

1  
2  
3  
4  
5  
6  
7  
8  
9  
10 810 field. The top of the Middle Jurassic Kashafrud Formation is marked by an  
11 811 important erosional surface and locally by an angular unconformity with the  
12  
13 812 overlying series.

14  
15 813 This Middle Jurassic rift system in the Kopet Dagh region has been coeval  
16  
17 814 with the South Caspian Sea rifting event (Brunet et al., 2003). From a  
18  
19 815 petroleum point of view, the Kashafrud Formation is considered as one of  
20  
21 816 the main source rocks of the Amu Darya Basin, but forms a bad reservoir,  
22  
23 817 because of early diagenesis (Poursoltani and Gibling, 2011).

24  
25  
26 818 *5.3. Late Jurassic / Early Cretaceous*

27  
28 819 The Upper-Jurassic to Early Cretaceous series observed in the Kopet  
29  
30 820 Dagh range also belong to the southern part of the Amu Darya Basin (Figure  
31  
32 821 18c). We infer the occurrence of gentle paleohighs in the eastern part of the  
33  
34 822 Kopet Dagh to explain variations in facies and thickness of the series from  
35  
36 823 the Upper Jurassic to the Lower Cretaceous. For example, to the North of  
37  
38 824 the Aghdarband erosional windows, Upper Jurassic Mozduran limestone is  
39  
40 825 reduced to few meters and there are no salt or evaporites above, in contrast  
41  
42 826 to the observations made in the Amu Darya Basin.

43  
44 827 From a petroleum point of view, the carbonates of the Mozduran Formation  
45  
46 828 as well as the clastics of the Shurijeh Formation are the main reservoirs of the  
47  
48 829 Amu Darya Basin. Towards the South, in the Kopet Dagh, there is no salt  
49  
50 830 on top of the Jurassic calcareous and the Upper Jurassic to Lower Cretaceous  
51  
52 831 series are thinner and more clastic.



1  
2  
3  
4  
5  
6  
7  
8  
9  
10  
11  
12  
13  
14  
15  
16  
17  
18  
19  
20  
21  
22  
23  
24  
25  
26  
27  
28  
29  
30  
31  
32  
33  
34  
35  
36  
37  
38  
39  
40  
41  
42  
43  
44  
45  
46  
47  
48  
49  
50  
51  
52  
53  
54  
55  
56  
57  
58  
59  
60  
61  
62  
63  
64  
65

832 *5.4. Late Cretaceous / Eocene*

833 In the northern and western parts of the Kopet Dagh range, several local  
834 erosional levels are observed (Figure 3). For example, a large hiatus from the  
835 late Barremian to the Santonian, as well as important thickness and facies  
836 variations are observed on the western cross-section (Figure 13). Further-  
837 more, the uppermost Cretaceous (Maastrichtian) is a stratigraphic hiatus,  
838 which is generalized in the whole Kopet Dagh region. Our results suggest  
839 several local tectonic uplifts in the southern part of the Amu Darya Basin  
840 during the Late Cretaceous (Figure 18d). The Paleocene series present im-  
841 portant facies variations from red continental series to carbonates across the  
842 belt whereas the Eocene Khangiran Formation marks the last marine episode  
843 recorded in the Amu Darya Basin and it does not present important thick-  
844 ness or facies variations.

845 Some authors report evidences for a Late Cretaceous-Paleocene compres-  
846 sion event in northern Iran (Barrier and Vrielynck, 2008) but this event is  
847 not well described at the moment. Notwithstanding, exhumation of the blue  
848 schist facies rocks within the Zagros belt and the exhumation of high-pressure  
849 rocks in the Sistan are broadly coincident with the obduction process of the  
850 Neotethyan lithosphere onto Arabia (Agard et al., 2011). Agard et al. (2011)  
851 propose that these exhumation phases could be the result of a regional-scale  
852 modification of plate-slab coupling in the Neotethys subduction zone during  
853 Late Cretaceous time. Further investigations in northern Iran are needed to  
854 better describe these compressive events.

1  
2  
3  
4  
5  
6  
7  
8  
9 855 *5.5. Late Eocene / Early Oligocene: onset of the Alpine orogeny*

10  
11 856 The thick-skin uplift and folding of the Kopet Dagh during the Alpine  
12  
13 857 orogeny may be related to reactivation of former Paleozoic or Cimmerian  
14  
15 858 fault systems (Figure 19a). This is suggested by the linear front of the  
16  
17 859 Eastern and Central Kopet Dagh structures, which diverges in the western  
18  
19 860 Kopet Dagh where they are influenced by the presence of the Paleotethys  
20  
21 861 suture zone and of the South Caspian rigid block to the NW. This thick-  
22  
23 862 skin deformation could be associated with a crustal thickening phase that  
24  
25 863 is observed from geophysical modeling (Jiménez-Munt et al., 2012; Robert  
26  
27 864 et al., in prep). During the main Alpine compressive phase, folding style  
28  
29 865 and structures vary laterally as a function of pre-existing structures, rock  
30  
31 866 behavior and mechanical stratigraphy (Figure 19a). In the southeastern part  
32  
33 867 of the Kopet Dagh, the Paleotethys suture zone and the inherited Paleozoic  
34  
35 868 trend of the Main Kopet Dagh Fault are parallel. These pre-existing struc-  
36  
37 869 tures probably control both the location of the Alpine Kopet Dagh uplift  
38  
39 870 and folding and the basement-involved tectonic style we observed. Some lo-  
40  
41 871 cal inversions of Middle Jurassic graben were also highlighted even though  
42  
43 872 evidences of force folding within the Upper Jurassic to Lower Cretaceous  
44  
45 873 (Barremian) series have been shown too. On top of the Barremian series,  
46  
47 874 several dcollements located within the thick Aptian-Albian marls lead to the  
48  
49 875 formation of the triangle zone. Quite similar structures have already been  
50  
51 876 described in Venezuela Andes (Colletta et al., 1997; Duerto et al., 2006, e.g.)  
52  
53 877 or in the frontal part of Longmen Shan range (Robert et al., 2010, e.g.).  
54  
55 878 Towards the West, the structures are dominated by the resistance contrast  
56  
57 879 between the rigid block formed by the basement of the South Caspian Sea

1  
2  
3  
4  
5  
6  
7  
8  
9  
10  
11  
12  
13  
14  
15  
16  
17  
18  
19  
20  
21  
22  
23  
24  
25  
26  
27  
28  
29  
30  
31  
32  
33  
34  
35  
36  
37  
38  
39  
40  
41  
42  
43  
44  
45  
46  
47  
48  
49  
50  
51  
52  
53  
54  
55  
56  
57  
58  
59  
60  
61  
62  
63  
64  
65

880 Basin and the weaker western part of the Kopet Dagh range that has been  
881 previously deformed by the Cimmerian orogeny. Indeed, this deformation  
882 contrast results in the indentation of the rigid South Caspian Sea region dur-  
883 ing the Alpine compression (Allen et al., 2003). The deformation style is  
884 characterized by the double vergence of deep-seated thrusts faults (Figure  
885 8) and important disharmonies within the Mesozoic levels. Fish-tail type  
886 structures with décollement levels within Jurassic or Cretaceous shale levels  
887 are suggested. In this part, there is not much evidence of reactivation of the  
888 normal faults associated to the Middle Jurassic rifting faults and numerous  
889 short-cuts have been observed.

890 Marine sediments up to the Late Eocene are folded with the underlying for-  
891 mation during the Alpine phase. Eocene sediments are clipped inside the  
892 synclines and are unconformably covered by post-Eocene series. Within the  
893 Kopet Dagh range, most of the Oligocene-Neogene series are discordant,  
894 but growth strata within the Oligocene-Neogene series were observed in the  
895 southeastern part of the belt. Further datings of these series are needed, but  
896 a Late Eocene-Early Oligocene age for onset of the Alpine orogeny within  
897 the Kopet Dagh belt can be proposed.

898 *5.6. Oligocene to Mid-Pliocene: Important subsidence in the South Caspian*  
899 *Sea Basin*

900 The rapid subsidence of the South Caspian Sea starts just after the Late  
901 Eocene-Early Oligocene compression folding that is responsible for the main  
902 uplift phase within the Kopet Dagh and the Alborz mountains (Allen et al.,  
903 2003; Brunet et al., 2003). Most of the authors agree that the basement of  
904 the South Caspian Sea is an oceanic crust resulting from the opening of a

1  
2  
3  
4  
5  
6  
7  
8  
9  
10 905 back-arc basin north of the Neotethyan arc (Brunet et al., 2003). According  
11 906 to Allen et al. (2003), the South Caspian Sea basement corresponds to a  
12  
13 907 resistant block with almost no internal deformation, playing an indenter role,  
14  
15 908 which could explain the arcuate shape of the surrounding fold-and-thrusts  
16  
17 909 belts (Alborz, Kopet Dagh, and Talysh). The important thickness of the  
18  
19 910 Caspian series is sealing the previously described structures in the western  
20  
21 911 Kopet Dagh. Progressive onlap of these Oligocene and Miocene series on  
22  
23 912 top of the unconformity is observed on seismic sections. The structures with  
24  
25 913 hydrocarbon discoveries that exist along the western coast of Turkmenistan  
26  
27 914 up to the Moghan Plain in Iran (Figure 1b) are associated with the deep shale  
28  
29 915 ridges of the Oligocene Maykop Formation. These arch structures correspond  
30  
31 916 to a Miocene proto Amu Darya delta in that region and the development  
32  
33 917 of shale ridge in the delta front during the Miocene. An increase of the  
34  
35 918 subsidence rate was observed during the latest Miocene and Pliocene periods  
36  
37 919 and the Amu Darya River shifted to a northward position. This new large  
38  
39 920 prograding system towards the South Caspian Sea Basin is associated with  
40  
41 921 the deposition of the Lower Pliocene main reservoirs. It cover nearly half of  
42  
43 922 the surface of the South Caspian Sea Basin with the development of a new  
44  
45 923 delta front oriented NE-SW in the central part of the basin.

46 924 *5.7. Mid-Pliocene to Present day: Indentation and onset of the extrusion in*  
47  
48 925 *the Kopet Dagh*

49  
50 926 Major changes of tectonic regime have been highlighted during the Plio-  
51  
52 927 Quaternary at the scale of the South Caspian Sea Basin and its surrounding  
53  
54 928 domains (Axen et al., 2001; Allen et al., 2004; Copley and Jackson, 2006;  
55  
56 929 Abbassi et al., 2009; Shabanian et al., 2009a) (Figure 19c). Moreover, con-

1  
2  
3  
4  
5  
6  
7  
8  
9  
10  
11  
12  
13  
14  
15  
16  
17  
18  
19  
20  
21  
22  
23  
24  
25  
26  
27  
28  
29  
30  
31  
32  
33  
34  
35  
36  
37  
38  
39  
40  
41  
42  
43  
44  
45  
46  
47  
48  
49  
50  
51  
52  
53  
54  
55  
56  
57  
58  
59  
60  
61  
62  
63  
64  
65

930 version from mainly thrusting to oblique-slip and strike-slip faulting within  
931 the Kopet Dagh range occurred during the late Cenozoic (~4-5 Ma) as a con-  
932 sequence of the major tectonic reorganization in NE Iran (Shabanian et al.,  
933 2009a,b). Ritz et al. (2006) suggested that a northwestward motion of the  
934 South Caspian Sea Basin compared to Eurasia and/or its clockwise rotation  
935 could explain this tectonic reorganization. Masson et al. (2006) proposed a  
936 second tectonic force due to the initiation of the northward subduction of  
937 the oceanic basement of the South Caspian Sea Basin below the Apsheron  
938 ridge.

939 In the Gorgan Plain and along the Turkmen margin of the Caspian Sea, the  
940 discordant series lying on top of the older series folded by the first Alpine  
941 phase are deformed too (Figure 15). This deformation implies a refolding  
942 of the unconformity by reactivation of the underlying structures. Oblique  
943 inversion of the Kashafrud grabens and strike-slip along the Main Kopet  
944 Dagh Fault, which extends from the South Caspian Sea to the Afghan bor-  
945 der are associated with this late deformation phase. En echelon pattern of  
946 the folds along this zone and en echelon fault pattern observed on 3D seismic  
947 blocks demonstrate a dextral shear component during the folding and inver-  
948 sion/reactivation. The importance of the strike-slip faults is demonstrated  
949 by the present-day seismicity across the range as well as by geomorphological  
950 data.

951 **6. Conclusions**

952 In this paper, we provide a detailed and revised characterization of the  
953 stratigraphy and the tectonics of the Kopet Dagh belt from new stratigraphic,

1  
2  
3  
4  
5  
6  
7  
8  
9  
10  
11  
12  
13  
14  
15  
16  
17  
18  
19  
20  
21  
22  
23  
24  
25  
26  
27  
28  
29  
30  
31  
32  
33  
34  
35  
36  
37  
38  
39  
40  
41  
42  
43  
44  
45  
46  
47  
48  
49  
50  
51  
52  
53  
54  
55  
56  
57  
58  
59  
60  
61  
62  
63  
64  
65

954 structural and seismic data. Based on these new data, we are able to define  
955 the tectonic history of the Kopet Dagh, which is most likely related with  
956 the adjacent South Caspian Sea and Amu Darya basins. We focused our  
957 study on the deformation recorded within the Kopet Dagh after the Cim-  
958 merian orogeny, which corresponds to the closure of the Paleotethys Ocean.  
959 The main unconformity that is widely described within the Kopet Dagh,  
960 is located at the base of the first deposited sediments after the Cimmerian  
961 orogeny: the Middle Jurassic Kashafrud Formation. We highlighted abrupt  
962 facies and thickness changes within the Middle Jurassic Kashafrud Forma-  
963 tion, as well as evidences of active rifting during the deposition of this forma-  
964 tion from seismic sections. The onset of deposition of the Amu Darya Basin  
965 corresponds to the Middle Jurassic synchronously to the initiation of active  
966 rifting.

967 Within the thick sedimentary sequence, we evidence several hiatus during the  
968 Cretaceous and the Paleocene in the northwestern part of the belt. These  
969 sedimentary hiatus highlight several local uplifts, suggesting a tectonic reac-  
970 tivation of the belt as early as during the Late Cretaceous/Paleocene. These  
971 local uplifts can be interpreted as the consequence of the distal closure of  
972 small oceanic domains, such as the Sistan Ocean. Finally, the onset of the  
973 Alpine compression occurred after the deposition of the marly Khangiran For-  
974 mation during the Eocene and resulted in the inversion of segments of the  
975 Jurassic-Cretaceous sedimentary basin and the reactivation of their bound-  
976 ing faults as well as newly created thrusts. Towards the South Caspian Sea  
977 Basin, we highlighted a major Late Eocene unconformity with progressive  
978 onlap above this unconformity, which indicates an age for the tectonic re-

1  
2  
3  
4  
5  
6  
7  
8  
9  
10  
11  
12  
13  
14  
15  
16  
17  
18  
19  
20  
21  
22  
23  
24  
25  
26  
27  
28  
29  
30  
31  
32  
33  
34  
35  
36  
37  
38  
39  
40  
41  
42  
43  
44  
45  
46  
47  
48  
49  
50  
51  
52  
53  
54  
55  
56  
57  
58  
59  
60  
61  
62  
63  
64  
65

979 activation of the belt as early as Late Eocene-Early Oligocene. In contrast,  
980 there is no precise timing for the activation of the Alpine tectonics in the  
981 eastern part of the belt. In the western part of the belt, the double-verging  
982 structures consist of thrust faults involving basement and fault-propagation  
983 folds within the sedimentary sequence. The entire succession until the Late  
984 Eocene is folded and newly-formed thrusts cross-cut the previous structures  
985 of the Middle Jurassic Kashafrud grabens. In the eastern part of the belt,  
986 this study demonstrates Middle Jurassic graben inversion with evidences  
987 of forced-folding and few short-cuts, as well by larger structures involving  
988 basement. Furthermore, seismic sections evidence several décollement levels  
989 within the Mesozoic sequence, which explains numerous disharmonies and  
990 fish-tails structures.

991 The important subsidence in the South Caspian Sea Basin began during  
992 the Early Oligocene and it is responsible for the sealing of the structures  
993 by the thick Oligocene to Quaternary sedimentary sequences in the western  
994 part of the belt. Finally, the tectonic reorganization in North Iran since the  
995 Pliocene is responsible for the dominance of the strike-slip component in the  
996 present-day deformation affecting the Kopet Dagh.

997 **7. Acknowledgments**

998 This study was funded by the Darius Consort2009bum and thanks to the  
999 strong support and collaboration with the National Iranian Oil Company  
1000 (NIOC). Additional funding was provided by the projects ATIZA(CGL2009-  
1001 09662-BTE) and TECLA (CGL201126670). The authors are very grateful  
1002 to geologists from the NIOC for their support during the field missions and

1  
2  
3  
4  
5  
6  
7  
8  
9 1003 for the help they provided in publishing this study.

10  
11  
12 1004 **References**

13  
14  
15 1005 Abbassi, A., Nasrabadi, A., Tatar, M., Yaminifard, F., Abbassi, M. R.,  
16  
17 1006 Hatzfeld, D., Priestley, K., 2009. Crustal velocity structure in the southern  
18  
19 1007 edge of the Central Alborz (Iran). *Journal of Geodynamics* 49, 68–78.

20  
21  
22 1008 Afshar-Harb, A., 1979. The stratigraphy, tectonics and petroleum geology of  
23  
24 1009 the Kopet Dagh Region, northern Iran. Ph.D. thesis, Imperial College of  
25  
26 1010 Science and Technology, University of London.

27  
28  
29 1011 Agard, P., Omrani, J., Jolivet, L., Whitechurch, H., Vrielynck, B., Spakman,  
30  
31 1012 W., Monié, P., Meyer, B., Wortel, R., 2011. Zagros orogeny: a subduction-  
32  
33 1013 dominated process. *Geol. Mag.* 148 (5-6), 692–725.

34  
35 1014 Aghanabati, A., 2004. *Geology of Iran*. Geological survey of Iran publication,  
36  
37 1015 558p.

38  
39  
40 1016 Alavi, M., 1992. Thrust tectonics of Binalood region, NE Iran. *Tectonics* 11,  
41  
42 1017 360–370.

43  
44 1018 Alavi, M., Vaziri, H., Emami, K. S., Lasemi, Y., 1997. The triassic and  
45  
46 1019 associated rocks of the Agh-Darband areas in central and northeastern  
47  
48 1020 Iran as remnant of the southern Turanian active continental margin. *GSA*  
49  
50 1021 *Bulletin* 109, 1563–1575.

51  
52  
53 1022 Allameh, M., Torshizian, H., Moradian, F., Amandar, B., 2010. Study of  
54  
55 1023 ostracodes in Abderaz Formation in Kopet-Dagh Basin, the 1st Interna-



1  
2  
3  
4  
5  
6  
7  
8  
9  
10  
11  
12  
13  
14  
15  
16  
17  
18  
19  
20  
21  
22  
23  
24  
25  
26  
27  
28  
29  
30  
31  
32  
33  
34  
35  
36  
37  
38  
39  
40  
41  
42  
43  
44  
45  
46  
47  
48  
49  
50  
51  
52  
53  
54  
55  
56  
57  
58  
59  
60  
61  
62  
63  
64  
65

1024 tional Applied Geological Congress, Department of Geology, Islamic Azad  
1025 University - Mashad Branch, Iran.

1026 Allen, M., Jackson, J., Walker, R., 2004. Late Cenozoic reorganization of the  
1027 Arabia-Eurasia collision and the comparison of short-term and long-term  
1028 deformation rates. *Tectonics* 23.

1029 Allen, M. B., Vincent, S. J., Alsop, G. I., Ismalail-zadeh, A., Flecker, R.,  
1030 2003. Late Cenozoic deformation in the South Caspian region: effects of a  
1031 rigid basement block within a collision zone. *Tectonophysics* 366, 223–239.

1032 Amurskiy, G. I., 1971. The deep structure of the Kopetdagh. *Geotectonics*  
1033 1, 34–40.

1034 Axen, G. J., Lam, P. S., Grove, M., Stockli, D. F., Hassanzadeh, J., 2001. Ex-  
1035 humation of the west-central Alborz Mountains, Iran, Caspian subsidence,  
1036 and collision-related tectonics. *Geology* 29 (6), 559–562.

1037 Barrier, E., Vrielynck, B., 2008. Palaeotectonic maps of the Middle East.  
1038 MEBE Programme. Atlas of 14 maps, CCGM.

1039 Baud, A., Stampfli, G., 1989. Tectonogenesis and evolution of a segment of  
1040 the Cimmerids: The volcano-sedimentary Triassic of Agh-Darband (Kopet  
1041 Dagh, North-East Iran). In: SENGOR, A.M.D., (Ed.): *Tectonic evolution*  
1042 *of the Tethyan Region*, Kluwer, Dordrec, 265–275.

1043 Berberian, M., 1983. The Southern Caspian: A compressional depression  
1044 floored by a trapped, modified oceanic crust. *Canadian Journal of Earth*  
1045 *Sciences* 20 (2), 163–183.

1  
2  
3  
4  
5  
6  
7  
8  
9  
10  
11  
12  
13  
14  
15  
16  
17  
18  
19  
20  
21  
22  
23  
24  
25  
26  
27  
28  
29  
30  
31  
32  
33  
34  
35  
36  
37  
38  
39  
40  
41  
42  
43  
44  
45  
46  
47  
48  
49  
50  
51  
52  
53  
54  
55  
56  
57  
58  
59  
60  
61  
62  
63  
64  
65

1046 Berberian, M., King, G. C. P., 1981. Towards a paleogeography and tectonic  
1047 evolution of iran. *Canadian Journal of Earth Sciences* 18, 1764–1766.

1048 Brunet, M.-F., Korotaev, M. V., Ershov, A. V., Nikishin, A. M., 2003. The  
1049 South Caspian Basin : a review of its evolution from subsidence modelling.  
1050 *Sedimentary Geology* 156, 119–148.

1051 Colletta, B., Roure, F., de Toni, B., Loureiro, D., 1997. Tectonic inheritance,  
1052 crustal architecture, and contrasting structural styles in the Venezuela  
1053 Andes. *Tectonics*.

1054 Copley, A., Jackson, J., 2006. Active tectonics of the Turkish-Iranian  
1055 plateau. *Tectonics* 25 (TC6006).

1056 Dikenshteyn, G., Maksimov, S., Semenovich, V., 1983. Petroleum provinces  
1057 of the URSS (Neftegazonosynye provintsii SSSR), moscow, Nedra, 272p.

1058 Duerto, L., Escalona, A., Mann, P., 2006. Deep structure of the Meacu-  
1059 terida Andes and Sierra de Perijaacute mountain fronts, Maracaibo Basin,  
1060 Venezuela. *AAPG Bulletin* 90 (4), 505–528.

1061 Emami, K. S., Fürsich, F. T., Wilmsen, M., 2004. Documentation and sig-  
1062 nificance of tectonic events in the northern Tabas block (East-central  
1063 Iran) during the Middle and Late Jurassic. *Revista Italica di Paleontologia*  
1064 *Stratigrafia* 110 (1), 163–171.

1065 Garzanti, E., Gaetani, M., 2002. Unroofing history of late Paleozoic mag-  
1066 matic arcs within the Turan Plate (Tuarkyr , Turkmenis tani). *Sedimen-  
1067 tary Geology* 151, 67–87.

1  
2  
3  
4  
5  
6  
7  
8  
9  
10  
11  
12  
13  
14  
15  
16  
17  
18  
19  
20  
21  
22  
23  
24  
25  
26  
27  
28  
29  
30  
31  
32  
33  
34  
35  
36  
37  
38  
39  
40  
41  
42  
43  
44  
45  
46  
47  
48  
49  
50  
51  
52  
53  
54  
55  
56  
57  
58  
59  
60  
61  
62  
63  
64  
65

1068 Golonka, J., 2004. Plate tectonic evolution of the southern margin of Eurasia  
1069 in the Mesozoic and Cenozoic. *Tectonophysics* 381, 235–273.

1070 Hollingsworth, J., Fattahi, M., Walker, R., Talebian, M., Bahroudi, A.,  
1071 Jackson, M. J., Copley, A., 2010. Oroclinal bending, distributed thrust  
1072 and strike-slip faulting, and the accommodation of Arabia-Eurasia conver-  
1073 gence in NE Iran since the Oligocene. *Geophysical Journal International*  
1074 181, 1214–1246.

1075 Hollingsworth, J., Jackson, J., Walker, R., Gheitanchi, M., Bolourchi, M.,  
1076 2006. Strike-slip faulting, rotation, and along-strike elongation in the  
1077 Kopeh dagh mountains, NE Iran. *Geophys. J. Int.* 166, 1161–1177.

1078 Hollingsworth, J., Jackson, J., Walker, R., Nazari, H., 2008. Extrusion tec-  
1079 tonics and subduction in the eastern South Caspian region since 10 Ma.  
1080 *Geology* 36 (10), 763–766.

1081 Hollingsworth, J., 2007. Active tectonics of NE Iran. Ph.D. thesis, Queen's  
1082 college, University of Cambridge.

1083 Jamali, F., Hessami, K., Ghorashi, M., 2011. Active tectonics and strain  
1084 partitioning along dextral fault system in Central Iran: analysis of ge-  
1085 omorphological observations and geophysical data in the Kashan region.  
1086 *Journal of Asian Earth Sciences* 40, 1015–1025.

1087 Jiménez-Munt, I., Fernández, M., Saura, E., Vergés, J., Garcia-Castellanos,  
1088 D., 2012. 3D lithospheric structure and regional/residual Bouguer anoma-  
1089 lies from Arabia-Eurasia collision in Iran. *Geophys. J. Int.* xxx.

1  
2  
3  
4  
5  
6  
7  
8  
9  
10  
11  
12  
13  
14  
15  
16  
17  
18  
19  
20  
21  
22  
23  
24  
25  
26  
27  
28  
29  
30  
31  
32  
33  
34  
35  
36  
37  
38  
39  
40  
41  
42  
43  
44  
45  
46  
47  
48  
49  
50  
51  
52  
53  
54  
55  
56  
57  
58  
59  
60  
61  
62  
63  
64  
65

1090 Kalantari, A., 1969. Foraminifera from the Middle Jurassic–Cretaceous suc-  
1091 cession of Kopet–dagh region. NIOC, Geological Laboratory Publication.

1092 Kavooosi, M., Lasemi, Y., Sherkati, S., Moussavi-Harami, R., 2009a. Fa-  
1093 cies analysis and depositional sequences of the Upper Jurassic Mozdu-  
1094 ran Formation, a reservoir in the Kopet Dagh Basin, NE iran. *Journal of*  
1095 *Petroleum Geology* 32 (3), 235–260.

1096 Kavooosi, M., Sepehr, M., Sherkati, S., 2009b. The kopet-dagh basin evolution  
1097 during middle-late jurassic. Extended abstracts EAGE Meeting, Shiraz,  
1098 Iran.

1099 Korotaev, M., Ershov, A., Nikishin, A., Brunet, M. F., 1999. Sedimentary  
1100 basins in compressional environment—modelling of the rapid subsidence.  
1101 EAGE Meeting, June, 1999, Helsinki, Finland. Extended abstract.

1102 Lyberis, N., Manby, G., 1999. Oblique to orthogonal convergence across the  
1103 Turan Block in the post-Miocene. *AAPG Bulletin* 83 (7), 1135–1160.

1104 Lyberis, N., Manby, G., Poli, J.-T., Kalougin, V., Yousouphocaev, H.,  
1105 Ashirov, T., 1998. Post-triassic evolution of the southern margin of the  
1106 Turan plate. *C.R. Acad. Sci. Paris* 326, 137–143.

1107 Maggi, M., Jackson, J., McKenzie, D., Priestley, K., 2000. Earthquake fo-  
1108 cal depths, effective elastic thickness, and the strength of the continental  
1109 lithosphere. *Geology* 28 (6), 495–498.

1110 Majadifard, M., 2003. Biostratigraphy, lithostratigraphy, ammonite taxon-  
1111 omy and microfacies analysis of the Middle and Upper Jurassic of north-

1  
2  
3  
4  
5  
6  
7  
8  
9  
10  
11  
12  
13  
14  
15  
16  
17  
18  
19  
20  
21  
22  
23  
24  
25  
26  
27  
28  
29  
30  
31  
32  
33  
34  
35  
36  
37  
38  
39  
40  
41  
42  
43  
44  
45  
46  
47  
48  
49  
50  
51  
52  
53  
54  
55  
56  
57  
58  
59  
60  
61  
62  
63  
64  
65

1112 eastern Iran. Ph.D. thesis, Der Bayerischen Julius-Maximilians-Universität  
1113 Würzburg.

1114 Martini, E., 1971. Standard Tertiary and Quaternary calcareous nanno-  
1115 plankton zonation. In: Second Planktonic Conference. Rome, pp. 739–785.

1116 Masson, F., Djamour, Y., Gorp, S. V., Chéry, J., Tatar, M., Tavakoli, F.,  
1117 Nankali, H., Vernant, P., 2006. Extension in NW Iran driven by the motion  
1118 of the South Caspian Basin. *Earth and Planetary Science Letters* 252, 180–  
1119 188.

1120 Moussavi-Harami, R., Brenner, R., 1990. Lower Cretaceous (Neocomian) flu-  
1121 vial deposits in eastern Kopet-Dagh Basin, northeastern Iran. *Cretaceous*  
1122 *Research* 11, 163–174.

1123 Moussavi-Harami, R., Brenner, R., 1992. Geohistory analysis and petroleum  
1124 reservoir characteristics of Lower Cretaceous (Neocomian) sandstones,  
1125 eastern Kopet Dagh Basin, northeastern Iran. *American Association of*  
1126 *Petroleum Geologists Bulletin* 76, 1200–1208.

1127 Moussavi-Harami, R., Mahboubi, A., Nadjafi, M., Brenner, R. L., Mortazavi,  
1128 M., 2009. Mechanism of calcrete formation in the Lower Cretaceous (Neo-  
1129 comian) fluvial deposits, northeastern Iran based on petrographic, geo-  
1130 chemical data. *Cretaceous Research* 30, 1146–1156.

1131 Muttoni, G., Mattei, M., Balini, M., Zanchi, A., Gaetani, A., Berra, F., 2009.  
1132 The drift history of Iran from the Ordovician to the Triassic. *Geological*  
1133 *Society of London, Special Publication: South Caspian to Central Iran*  
1134 *Basins* 312, 7–29.

1  
2  
3  
4  
5  
6  
7  
8  
9  
10  
11  
12  
13  
14  
15  
16  
17  
18  
19  
20  
21  
22  
23  
24  
25  
26  
27  
28  
29  
30  
31  
32  
33  
34  
35  
36  
37  
38  
39  
40  
41  
42  
43  
44  
45  
46  
47  
48  
49  
50  
51  
52  
53  
54  
55  
56  
57  
58  
59  
60  
61  
62  
63  
64  
65

1135 Perch-Nielsen, K., 1985. Mesozoic calcareous nannofossils, in Bolli, H.M.,  
1136 Saunders, J.B., and Perch-Nielsen. *Plankton Stratigraphy*: Cambridge,  
1137 Cambridge University Press, 330–426.

1138 Poursoltani, M. R., Gibling, M. R., 2011. Composition, porosity, and reser-  
1139 voir potential of the Middle Jurassic Kashafrud Formation, northeast Iran.  
1140 *Marine and Petroleum Geology* 28 (5), 1094 – 1110.

1141 Poursoltani, M. R., Moussavi-Harami, S. R., Gibling, M. R., 2007. Jurassic  
1142 deep-water fans in the Neo-Tethys Ocean: The Kashafrud Formation of  
1143 the Kopet-Dagh basin, Iran. *Sedimentary Geology* 198 (1), 53–74.

1144 Raisossadat, S. N., Shokri, M. H., 2011. Biostratigraphic studies of the  
1145 Lower Cretaceous (Upper Barremian—Lower Aptian) Sarcheshmeh and  
1146 Sanganeh formations in the Kopet Dagh basin, NE Iran: An integration  
1147 of calcareous nannofossil and ammonite stratigraphies. *Stratigraphy and  
1148 Geological Correlation* 19 (2), 188–204.

1149 Reilinger, R., McClusky, S., Vernant, P., Lawrence, S., Ergintav, S., Cak-  
1150 mak, R., Ozener, H., Kadirov, F., Guliev, I., Stepanyan, R., Nadariya,  
1151 M., Hahubia, G., Mahmoud, S., Sakr, K., ArRajehi, A., Paradissis, D.,  
1152 Al-Aydrus, A., Prilepin, M., Guseva, T., Evren, E., Dmitrotsa, A., Fil-  
1153 ikov, S., Gomez, F., Al-Ghazzi, R., Karam, G., 2006. GPS constraints on  
1154 continental deformation in the Africa-Arabia-Eurasia continental collision  
1155 zone and implications for the dynamics of plate interactions. *Journal of  
1156 Geophysical Research B: Solid Earth* 111 (5).

1157 Ritz, J.-F., Nazari, H., Ghassemi, A., Salamati, R., Shafei, A., Solaymani,

1  
2  
3  
4  
5  
6  
7  
8  
9  
10  
11  
12  
13  
14  
15  
16  
17  
18  
19  
20  
21  
22  
23  
24  
25  
26  
27  
28  
29  
30  
31  
32  
33  
34  
35  
36  
37  
38  
39  
40  
41  
42  
43  
44  
45  
46  
47  
48  
49  
50  
51  
52  
53  
54  
55  
56  
57  
58  
59  
60  
61  
62  
63  
64  
65

1158 S., Vernant, P., 2006. Active transtension inside central Alborz: a new in-  
1159 sight into northern Iran–southern Caspian geodynamics. *Geology* 34 (6),  
1160 477–480.

1161 Robert, A., Jiménez-Munt, I., Fernàndez, M., Vergés, J., in prep. Litho-  
1162 spheric structures in Central Eurasia derived from elevation, geoid anomaly  
1163 and a thermal analysis. *Geochemistry, Geophysics, Geosystems*.

1164 Robert, A., Pubellier, M., de Sigoyer, J., Vergne, J., Lahfid, A., Cattin,  
1165 R., Findling, N., Zhu, J., 2010. Structural and thermal characters of the  
1166 Longmen Shan (Sichuan, China). *Tectonophysics* 491 (1-4), 165–173.

1167 Ruttner, A., 1991. The Triassic of Aghdarband (AgDarband), NE-Iran, and  
1168 its pre-Triassic frame. *Abhandlungen der Geologischen Bundesanstalt* 38,  
1169 252p.

1170 Sengor, A. M. C., 1990. A new model for the late Palaeozoic–Mesozoic tec-  
1171 tonic evolution of Iran and implications for Oman. *Geological Society of*  
1172 *London, Special Publications* 49, 797–831.

1173 Shabanian, E., Bellier, O., Siame, L., Abbassi, M. R., Bourlès, D., Braucher,  
1174 R., Farbod, Y., 2012. The Binalud Mountains: A key piece for the geody-  
1175 namic puzzle of NE iran. *Tectonics* 31 (TC6003).

1176 Shabanian, E., Bellier, O., Siame, L., Arnaud, N., Abbassi, M. R., Cochemé,  
1177 J.-J., 2009a. New tectonic configuration in NE Iran: Active strike-slip  
1178 faulting between the Kopet Dagh and Binalud mountains. *Tectonics*  
1179 28 (TC5002).

- 1  
2  
3  
4  
5  
6  
7  
8  
9  
10 1180 Shabanian, E., Siame, L., Bellier, O., Benedetti, L., Abbassi, M. R., 2009b.  
11 Quaternary slip rates along the northeastern boundary of the Arabia–  
12 Eurasia collision zone (Kopeh Dagh Mountains, Northeast Iran). *Geophys-*  
13 *ical Journal International* 178, 1055–1077.  
14  
15  
16  
17  
18 1184 Shahidi, A., 2008. Evolution tectonique du Nord de l’Iran (Alborz et Kopet  
19 Dagh) depuis le Mésozoïque. Ph.D. thesis, Université Pierre et Marie Curie  
20 - Paris VI.  
21  
22  
23  
24 1187 Sharafi, m., ashuri, m., Mahboubi, A., Moussavi Harami, S. R., December  
25 2012. Stratigraphic application of *Thalassinoides* ichnofabric in delineat-  
26 ing sequence stratigraphic surfaces (Mid-Cretaceous), Kopet-Dagh Basin,  
27 northeastern Iran. *Palaeoworld* 21 (3), 202–216.  
28  
29  
30  
31  
32 1191 Sheikholeslami, M., Kouhpeym, M., 2012. Structurale analysis and tectonic  
33 evolution of the eastern Binalud Mountains, NE Iran. *Journal of Geody-*  
34 *namics* 61, 23–46.  
35  
36  
37  
38  
39 1194 Taheri, J., Fürsich, F., Wilmsen, M., 2009. Stratigraphy, depositional envi-  
40 ronments and geodynamic significance of the Upper Bajocian Bathonian  
41 Kashafrud Formation, NE Iran. *Geological Society of London, Special Pub-*  
42 *lication, South Caspian to Central Iran Basins* 312, 205–218.  
43  
44  
45  
46  
47  
48 1198 Tavakoli, F., 2007. Present-day deformation and kinematics of the active  
49 faults observed by GPS in the Zagros and East of Iran. Ph.D. thesis, Uni-  
50 versité Joseph Fourier - Grenoble I.  
51  
52  
53  
54 1201 Thierstein, H. R., 1976. Mesozoic calcareous nannoplankton biostratigraphy  
55 of marine sediments. *Marine Micropaleontology* 1, 325–362.  
56  
57  
58  
59  
60  
61  
62  
63  
64  
65



1  
2  
3  
4  
5  
6  
7  
8  
9  
10  
11  
12  
13  
14  
15  
16  
17  
18  
19  
20  
21  
22  
23  
24  
25  
26  
27  
28  
29  
30  
31  
32  
33  
34  
35  
36  
37  
38  
39  
40  
41  
42  
43  
44  
45  
46  
47  
48  
49  
50  
51  
52  
53  
54  
55  
56  
57  
58  
59  
60  
61  
62  
63  
64  
65

1203 Thomas, J., Cobbold, P., Shein, V., Douaran, S. L., 1999. Sedimentary record  
1204 of Late Paleozoic to recent tectonism in Central Asia—analysis of subsurface  
1205 data from the Turan and South Kazakh domains. *Tectonophysics* 313, 243–  
1206 263.

1207 Ulmishek, G. F., 2001. Petroleum geology and resources of the Middle  
1208 Caspian basin, former Soviet Union. U.S. Geological Survey Bulletin 99,  
1209 116p.

1210 Ulmishek, G. F., 2004. Petroleum geology and resources of the Amu-Darya  
1211 Basin, Turkmenistan, Uzbekistan, Afghanistan, and Iran. U.S. Geological  
1212 Survey Bulletin 2201-4, 32p.

1213 Vernant, P., Nilforoushan, F., Hatzfeld, D., Abbassi, M. R., Vigny, C., Mas-  
1214 son, F., Nankali, H., Martinod, J., Ashtiani, A., Bayer, R., Tavakoli, F.,  
1215 Chery, J., 2004. Present-day crustal deformation and plate kinematics in  
1216 the Middle East constrained by GPS measurements in Iran and northern  
1217 Oman. *Geophys. J. Int* 157, 381–398.

1218 Wilmsen, M., Fürsich, T., Emami, K. S., Majidifard, M. R., Taheri, M. R.,  
1219 2009. The Cimmerian Orogeny in northern Iran: tectono-stratigraphic ev-  
1220 idence from the foreland. *Terra Nova* 21, 221–218.

1221 Zanchetta, S., Berra, F., Zanchi, A., Bergomi, M., Caridroit, M., Nicorab,  
1222 A., Heidarzadeh, G., 2013. The record of the Late Palaeozoic active margin  
1223 of the Palaeotethys in NE Iran: Constraints on the Cimmerian orogeny.  
1224 *Gondwana Research* 24 (3-4), 1237–1266.

- 1  
2  
3  
4  
5  
6  
7  
8  
9  
10 1225 Zanchi, A., Balini, M., Ghassemi, M. R., Zanchetta, S., 2-7 May 2010. Mech-  
11 1226 anism of calcrete formation in the Lower Cretaceous (Neocomian) fluvial  
12 1227 deposits, northeastern Iran based on petrographic, geochemical data, EGU  
13 1228 General Assembly.
- 14  
15  
16  
17 1229 Zanchi, A., Berra, A., Mattei, M., Ghasemi, M. R., Sabouri, J., 2006. Inver-  
18 1230 sion tectonics in Central Alborz, Iran. *Journal of Structural Geology* 28,  
19 1231 2023–2037.
- 20  
21  
22  
23 1232 Zanchi, A., Zanchetta, S., Berra, F., Mattei, M., Garzanti, E., Molyneux,  
24 1233 S., Nawab, A., Sabouri, J., 2009. The Eo-Cimmerian (Late? Triassic)  
25 1234 orogeny in North Iran. *Geological Society of London, Special Publications*  
26 1235 312, 31–55.

27  
28  
29  
30  
31  
32  
33 Figure 1: a. Topographic map (ETOPO 1 data) of Iran showing the main tectonic units  
34 with location of the main volcanic rocks, salt and ophiolites outcrops. Neotethys and  
35 Paleotethys sutures zones are indicated. MKF: Main Kopet Dagh Fault; GKF: Great  
36 Kavir Fault; GKB: Great Kavir Basin; ABS: Apsheron-Balkhan System b. Topographic  
37 map of the Kopet Dagh range from ASTER GDEM data showing the location of the  
38 gas and oil fields (red area) from publications (Dikenshteyn et al., 1983; Ulmishek, 2004)  
39 and from the Oil and Gas Infrastructure in the Caspian Sea region, March 2001 from the  
40 United State Government. The Paleotethys suture zone and major places are indicated  
41 on this map. Major gas fields: 1: Dauletabad; 2: Gonbadli; 3: Khangiran; 4: Shaltyk; 5:  
42 Bayram-Ali; 6: Achak  
43  
44  
45  
46  
47  
48  
49  
50  
51  
52  
53  
54  
55  
56  
57  
58  
59  
60  
61  
62  
63  
64  
65

1  
2  
3  
4  
5  
6  
7  
8  
9  
10  
11  
12  
13  
14  
15  
16  
17  
18  
19  
20  
21  
22  
23  
24  
25  
26  
27  
28  
29  
30  
31  
32  
33  
34  
35  
36  
37  
38  
39  
40  
41  
42  
43  
44  
45  
46  
47  
48  
49  
50  
51  
52  
53  
54  
55  
56  
57  
58  
59  
60  
61  
62  
63  
64  
65

Figure 2: Seismotectonic map of the Kopet Dagh region where the major recent faults are represented according to (Hollingsworth et al., 2006; Hollingsworth, 2007; Hollingsworth et al., 2008, 2010; Shabanian et al., 2009a,b, 2012). Blue arrows represent GPS velocities relative to Eurasia fixed; the error ellipses indicate formal errors within 95 percent confidence interval (Tavakoli, 2007). The location of the Paleotethys suture zone is indicated. Focal mechanisms are taken from CMT Harvard catalogue for the period 1976-2012. The shaded relief background has been made from ASTER GDEM data. DF: Doruneh Fault; KF: Khazar Fault; MKF: Main Kopet Dagh Fault; NFS: Neyshabur Fault System.

Figure 3: New stratigraphic chart of the Kopet Dagh belt and of two main adjacent Amu Darya and South Caspian Sea basins. This stratigraphic study has been constructed from our 159 biostratigraphic datings, sedimentologic observations and a wide compilation of published data. Major tectonic events are been indicated on this stratigraphic chart and can be correlated with the main regional observed hiatus.

Figure 4: a) Prograding sequence of limestones belonging to the Upper Jurassic Mozduran Formation within the upper part of the upper Jurassic shally Chaman Bid Formation b) Clastic filling between 2 reefs within the Upper Jurassic Mozduran Formation. Similar features have been observed on seismic sections as highlighted in Figure 10.

Figure 5: Simplified geological map of the Kopet Dagh area compiled from the geological maps of the Geological Survey of Iran. Locations of the 4 regional cross-sections presented in this article are indicated.

1  
2  
3  
4  
5  
6  
7  
8  
9  
10  
11  
12  
13  
14  
15  
16  
17  
18  
19  
20  
21  
22  
23  
24  
25  
26  
27  
28  
29  
30  
31  
32  
33  
34  
35  
36  
37  
38  
39  
40  
41  
42  
43  
44  
45  
46  
47  
48  
49  
50  
51  
52  
53  
54  
55  
56  
57  
58  
59  
60  
61  
62  
63  
64  
65

Figure 6: The Aghdarband-Gonbadly cross-section (see location of the cross-section in Figure 5. This cross-section shows structural relationships between the rocks deformed by the Hercynian and/or the Cimmerian orogeny that outcrop in the Aghdarband erosional windows and the series deposited in the southwestern part of the Amu Darya Basin affected by the Alpine inversion of the Middle Jurassic extensional structures. Locations of the seismic data presented in this article and borehole data are indicated.

Figure 7: Tectonic sketch of the Aghdarband erosional window, modified from previous published cross-sections (Ruttner, 1991; Zanchi et al., 2010). The folded Triassic and older series are preserved below double verging thrusts. The deformed rocks are overlain by the Middle Jurassic Kashafrud Formation characterized by its basal conglomerate (J2). D: Devonian, C: Carboniferous, PT: Permo-Triassic molassic sediments, T1 and T2: part of the Triassic series (see description in the text), T3a: Triassic Miankuhi Formation, J2: Conglomeratic base of the Middle Jurassic Kashafrud Formation and J3: Upper part of the Middle Jurassic Kashafrud Formation.

Figure 8: Seismic section showing the triangle structure to the NW of the Aghdarband erosional window (location on the Aghdarband cross-section, Figure 6). This seismic line shows two major North-directed basement thrusts that branch into an inferred detachment within the shales of the Campanian. For calibration, we used field data and information from the borehole represented in the figure. Legend of the horizons: Black = Top Trias; Dark blue = top Kashafrud Formation (Middle Jurassic); Light blue = top Mozduran Formation (Upper Jurassic); Dark green = Top Shurijeh Formation (Neocomian); Green = Top Aitamir Formation (Cenomanian); Light green = Top Kalat Formation (Uppermost Cretaceous); Orange = Top Chehel Kaman Formation (Paleocene).

1  
2  
3  
4  
5  
6  
7  
8  
9  
10  
11  
12  
13  
14  
15  
16  
17  
18  
19  
20  
21  
22  
23  
24  
25  
26  
27  
28  
29  
30  
31  
32  
33  
34  
35  
36  
37  
38  
39  
40  
41  
42  
43  
44  
45  
46  
47  
48  
49  
50  
51  
52  
53  
54  
55  
56  
57  
58  
59  
60  
61  
62  
63  
64  
65

Figure 9: a) Seismic section from the Gonbadli gas field area (location in Figure 5) showing large-scale basement uplift. The Jurassic structure is shown by opposite set of normal faults, some of which seem to preserve their original normal displacement. b) Zoom on the previous seismic transect with a flattening done at the top Middle Jurassic horizon which highlight of the Kashafrud half graben structures. Legend of the horizons: Purple = Top Trias; Dark blue = top Kashafrud Formation (Middle Jurassic); Light blue = top Mozduran Formation (Upper Jurassic); Dark green = Top Shurijeh Formation (Neocomian); Green = Top Aitamir Formation (Cenomanian); Light green = Top Kalat Formation (Uppermost Cretaceous); Orange = Top Chehel Kaman Formation (Paleocene).

Figure 10: Seismic section across the Khangiran gas field extracted from a 3D cube. The Khangiran structure is due to the Tertiary inversion of a Middle Jurassic half graben. The occurrence of growth strata within the Oligocene-Neogene sequences highlights that the graben inversion is associated to the Alpine tectonic phase as a consequence of an inversion tectonics. The black arrow highlights some carbonate build-ups within the Upper Jurassic Mozduran limestones. Legend of the horizons: Purple = Top Trias; Dark blue = top Kashafrud Formation (Middle Jurassic); Light blue = top Mozduran Formation (Upper Jurassic); Dark green = Top Shurijeh Formation (Neocomian); Green = Top Aitamir Formation (Cenomanian); Light green = Top Kalat Formation (Uppermost Cretaceous); Orange = Top Chehel Kaman Formation (Paleocene); Yellow = Intra Oligo-Neogene conglomerates.

Figure 11: The Darre Gaz regional cross-section (see location in Figure 5) shows the inversion of Middle Jurassic front of the belt is characterized by North-verging basement thrusts that mostly branch into a major detachment within the Aptian-Albian series.

1  
2  
3  
4  
5  
6  
7  
8  
9  
10  
11  
12  
13  
14  
15  
16  
17  
18  
19  
20  
21  
22  
23  
24  
25  
26  
27  
28  
29  
30  
31  
32  
33  
34  
35  
36  
37  
38  
39  
40  
41  
42  
43  
44  
45  
46  
47  
48  
49  
50  
51  
52  
53  
54  
55  
56  
57  
58  
59  
60  
61  
62  
63  
64  
65

Figure 12: Seismic section showing typical structures of the Darre Gaz area with a disharmony between deep and surface structures implying several décollement levels within the Cretaceous series. The deeper horizons of this section are not calibrated. Legend of the horizons: Black = Top Trias; Dark blue = top Kashafrud Formation (Middle Jurassic); Light blue = top Mozduran Formation (Upper Jurassic); Dark green = Top Shurijeh Formation (Neocomian); Green = Top Aitamir Formation (Cenomanian); Light green = Top Kalat Formation (Uppermost Cretaceous); Orange = Top Chehel Kaman Formation (Paleocene).

Figure 13: The western regional cross-section (see location in Figure 5) highlights the upper basement décollement level forming double-verging structures that cross-cut the Middle Jurassic rift system. This cross-section also shows two folded unconformities: at the base of the Lower Cretaceous and at the base of the post-Eocene sediments.

Figure 14: Scheme of several fields observations highlighting the structural relationships between the different stratigraphic formations. The important thickness variations of the Middle Jurassic Kashafrud Formation is due to active rifting during deposition. An erosional surface at the base of the Late Jurassic Chaman Bid Formation and several progradations of the Upper Jurassic Mozduran limestones into the marls of the Late Jurassic Chaman Bid Formation are observed. Notice the reduced thickness of Cretaceous and Tertiary series.

1  
2  
3  
4  
5  
6  
7  
8  
9  
10  
11  
12  
13  
14  
15  
16  
17  
18  
19  
20  
21  
22  
23  
24  
25  
26  
27  
28  
29  
30  
31  
32  
33  
34  
35  
36  
37  
38  
39  
40  
41  
42  
43  
44  
45  
46  
47  
48  
49  
50  
51  
52  
53  
54  
55  
56  
57  
58  
59  
60  
61  
62  
63  
64  
65

Figure 15: The Gorgan Plain regional cross-section (see location in Figure 5) shows the buried folds of the Kopet Dagh beneath the thick post-Eocene sediments belonging to the South Caspian Sea Basin. This cross-section has mainly been constructed from seismic sections.

Figure 16: Seismic section below the Gorgan Plain to the Western part of the Kopet Dagh. This section shows the folded structures overlain by a major unconformity with progressive onlap above this unconformity. The pink horizon near the top of the section corresponds to the top of the Mid-Pleistocene strata, the red horizon corresponds to the Late-Eocene and Early Oligocene unconformity, the green horizons correspond to the Late Cretaceous marls and clastic sediments. Within the syncline, it is possible that the Paleogene up to the Upper Eocene were preserved. (a) Folded and faulted structures, the folds are oriented NE-SW parallel to the orientation of the western part of the Kopet Dagh belt (b) The red line corresponds to the folded unconformity at the base of the Oligocene-Neogene strata.

1  
2  
3  
4  
5  
6  
7  
8  
9  
10  
11  
12  
13  
14  
15  
16  
17  
18  
19  
20  
21  
22  
23  
24  
25  
26  
27  
28  
29  
30  
31  
32  
33  
34  
35  
36  
37  
38  
39  
40  
41  
42  
43  
44  
45  
46  
47  
48  
49  
50  
51  
52  
53  
54  
55  
56  
57  
58  
59  
60  
61  
62  
63  
64  
65

Figure 17: Seismic profile of the margin of the Caspian Sea Basin below the Gorgan Plain. Notice the unconformity highlighted in red which is covered by sediments of the South Caspian Sea Basin. A shale ridge structure is marked in red (M?) suggesting that the sediments just on top of the unconformity are probably made of the Oligocene Maykop Formation. The pink horizon corresponds to the near top Mid-Pleistocene, the yellow horizon corresponds to the near top Miocene, the red horizon corresponds to the Late Eocene-Early Oligocene unconformity and the green horizons correspond to the Late Cretaceous.

Figure 18: Schematic reconstructions of the geodynamic settings of the region centered on Central Iran during a) the Late Triassic to the Early Jurassic; b) the Middle Jurassic; c) the latest Jurassic to the Early Cretaceous and d) the Late Cretaceous to the Eocene. Reconstructions for the Neotethys and Iran were adapted from Agard et al. (2011); Barrier and Vrielynck (2008).

Figure 19: Schematic reconstructions of the geodynamic settings of the region centered on Central Iran during a) the Late Eocene to the Early Oligocene; b) the Oligocene to the Middle Pliocene and c) the Late Pliocene to the present-day. Reconstructions for the Neotethys and Iran were adapted from Agard et al. (2011); Barrier and Vrielynck (2008).



Figure 1  
[Click here to download high resolution image](#)

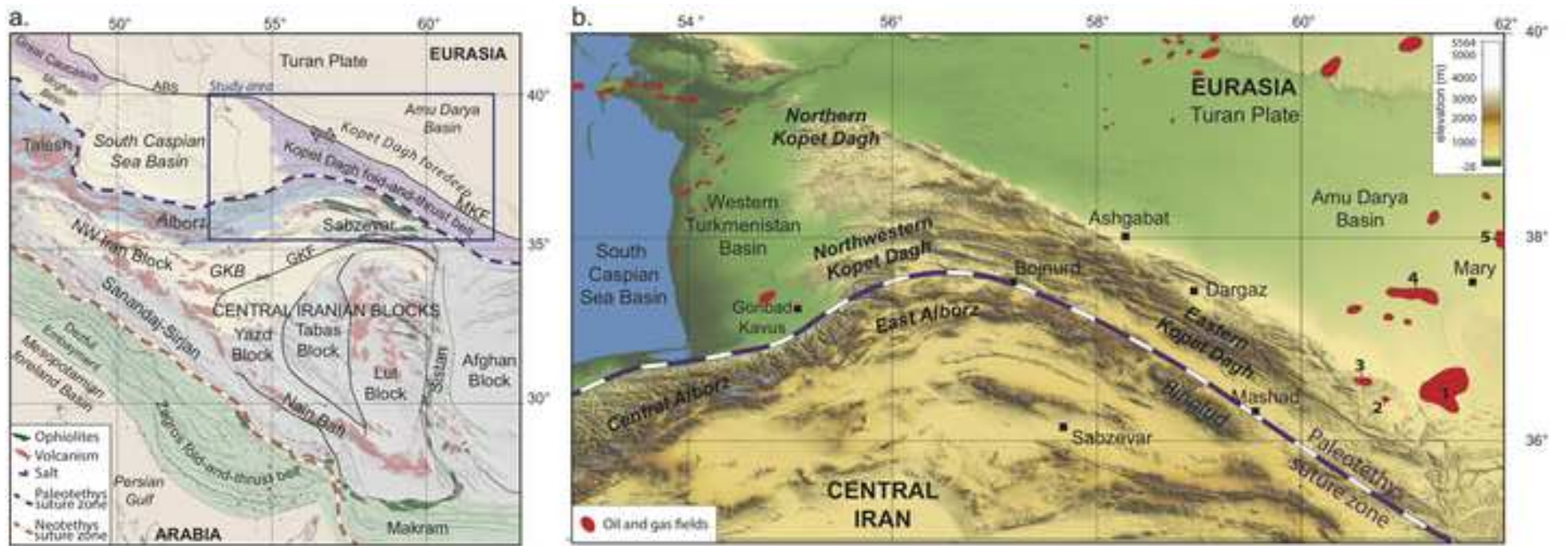
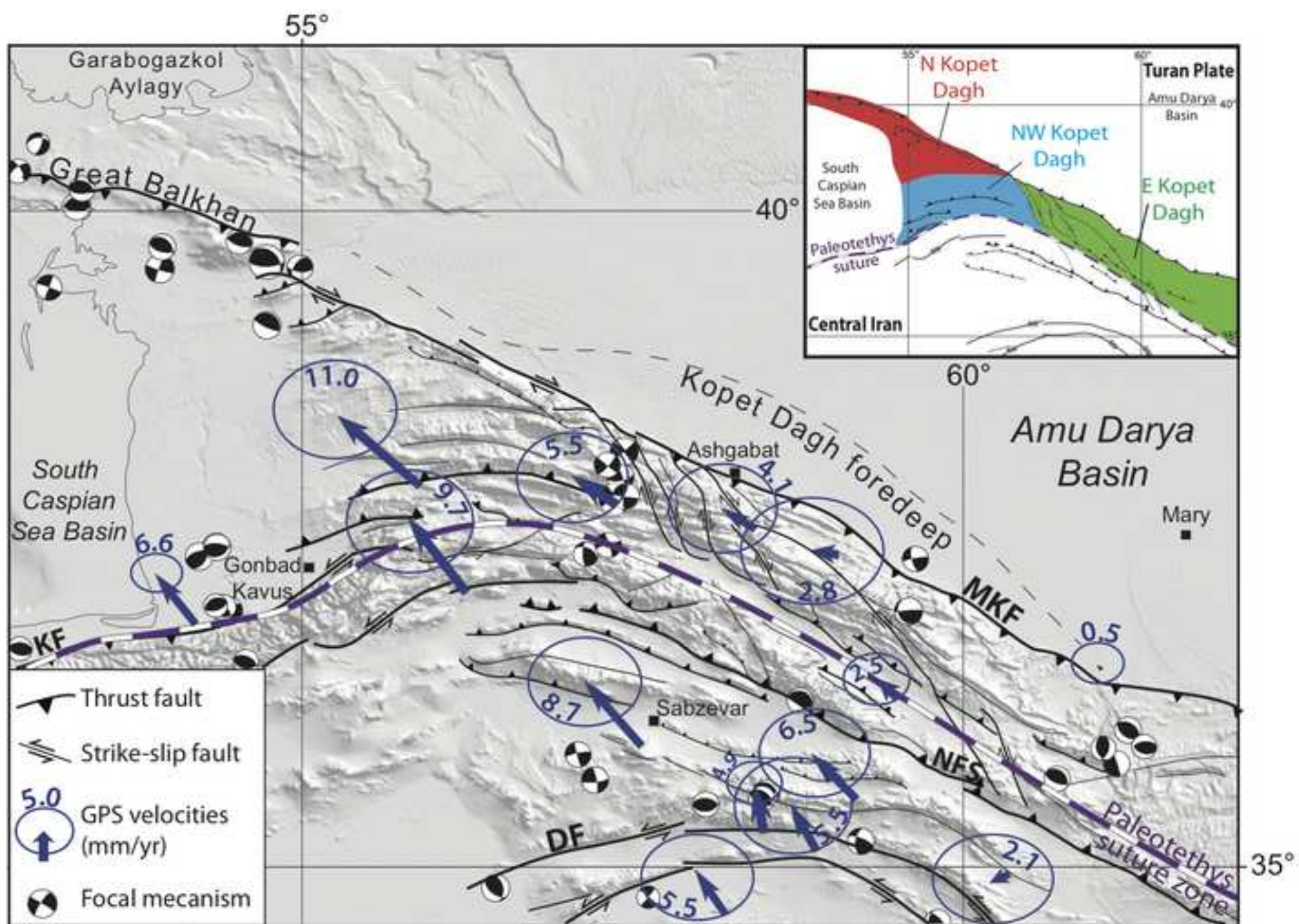


Figure 2  
[Click here to download high resolution image](#)





**Figure 3**

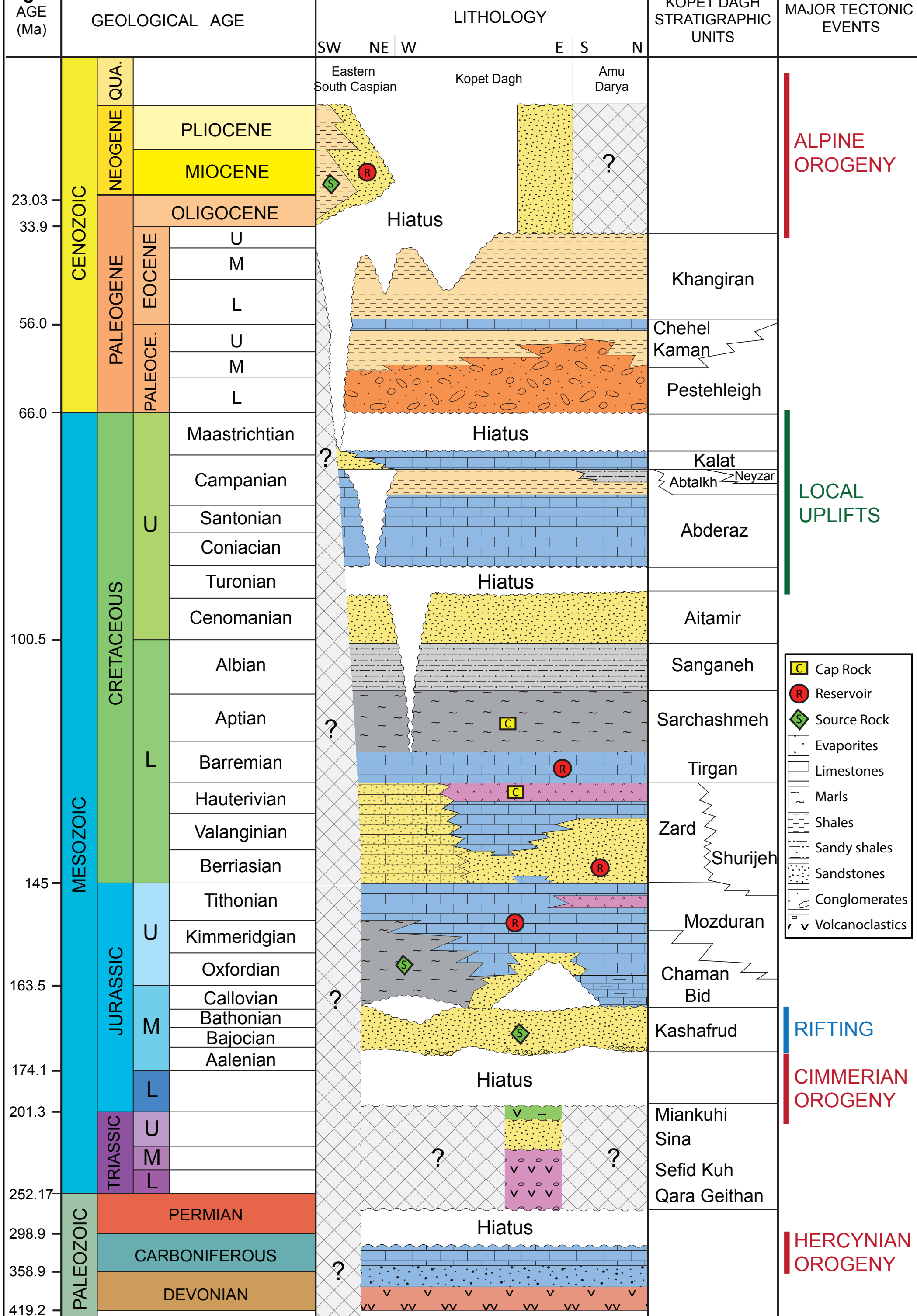


Figure 4  
[Click here to download high resolution image](#)

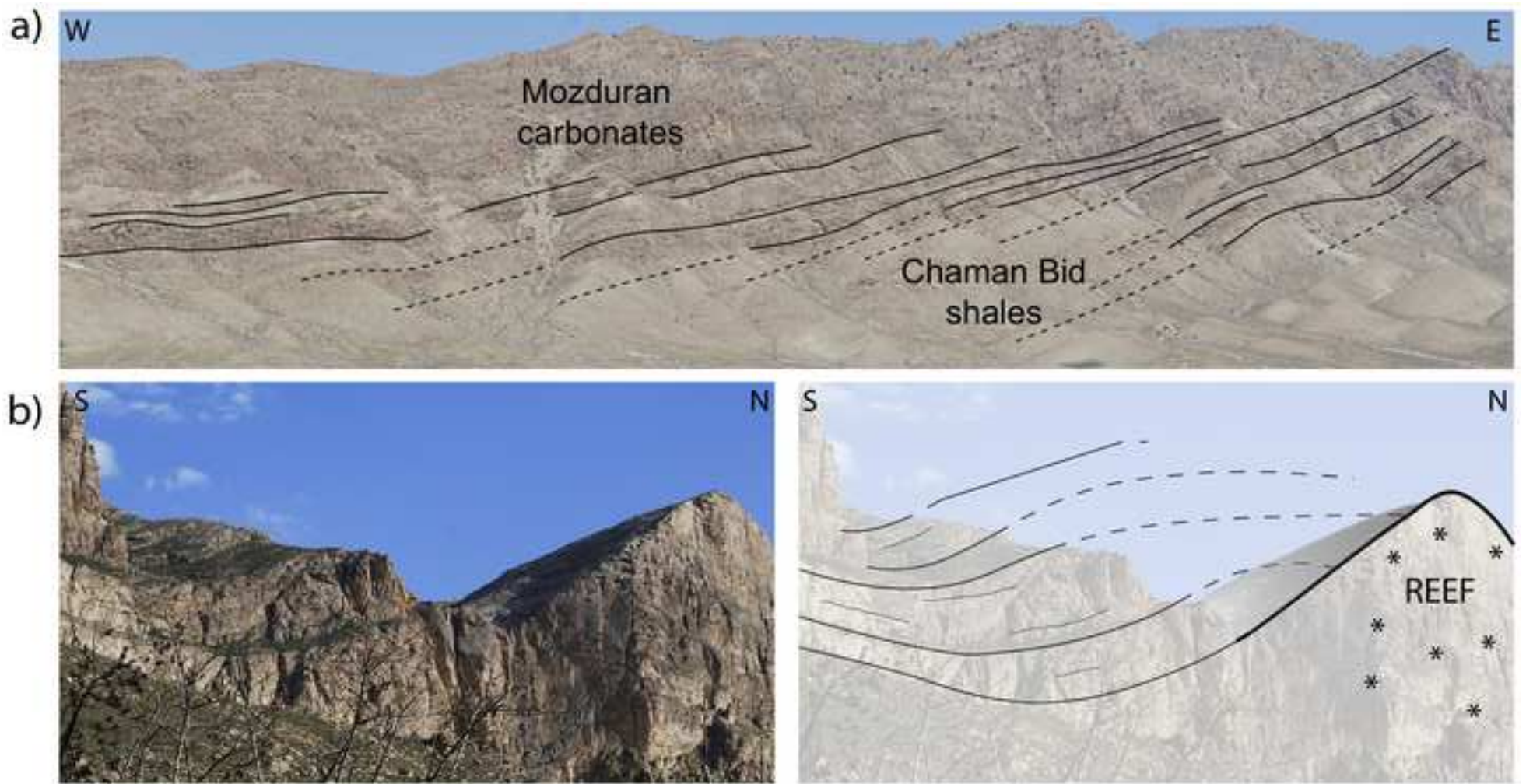


Figure 5

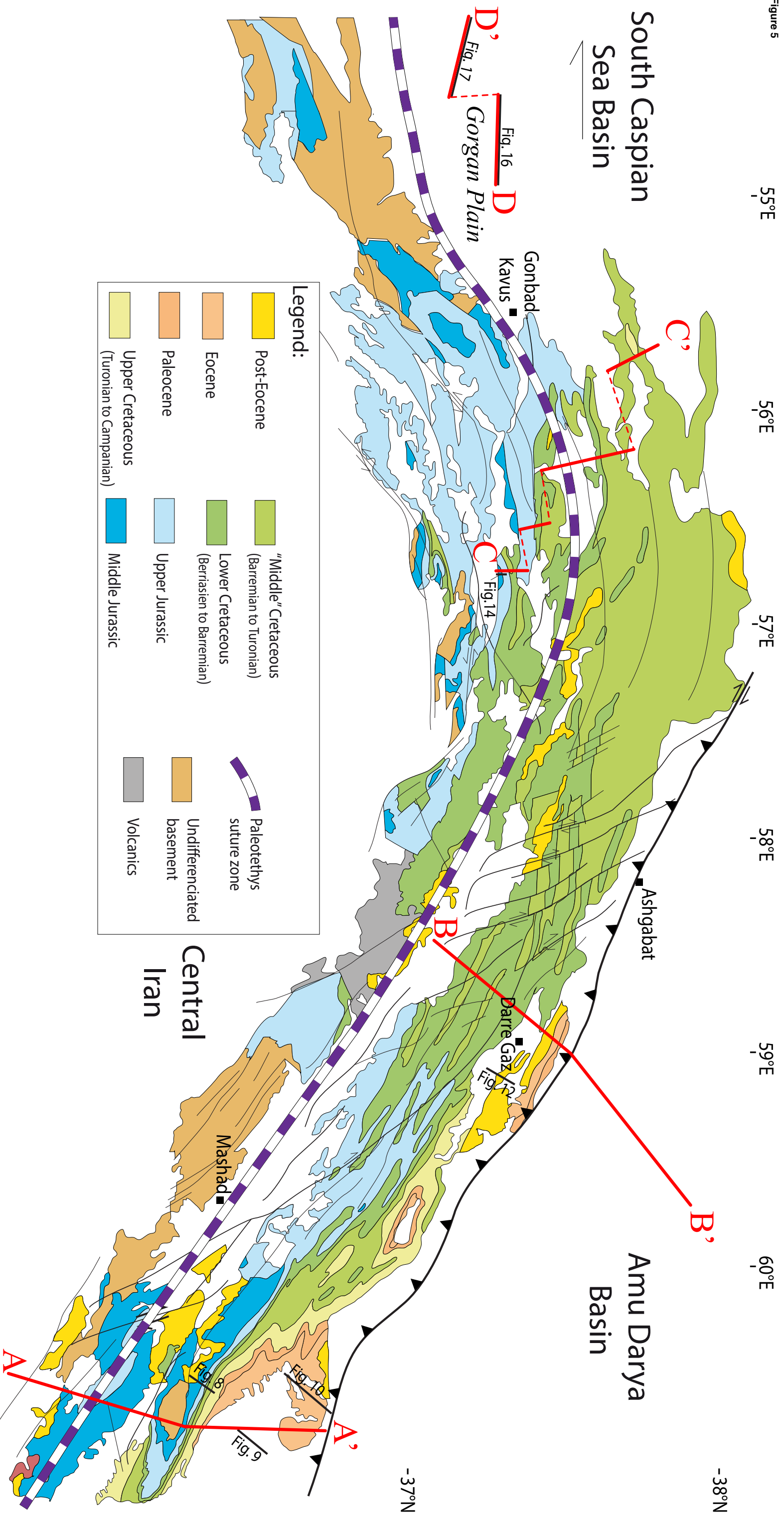




Figure 6  
[Click here to download high resolution image](#)

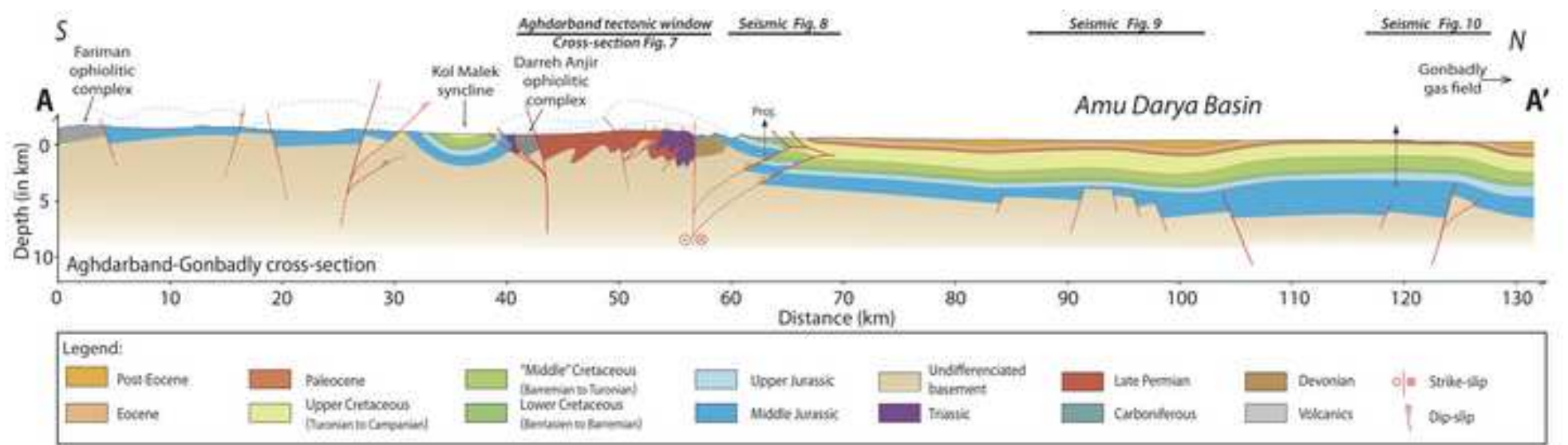


Figure 7  
SSW

NNE

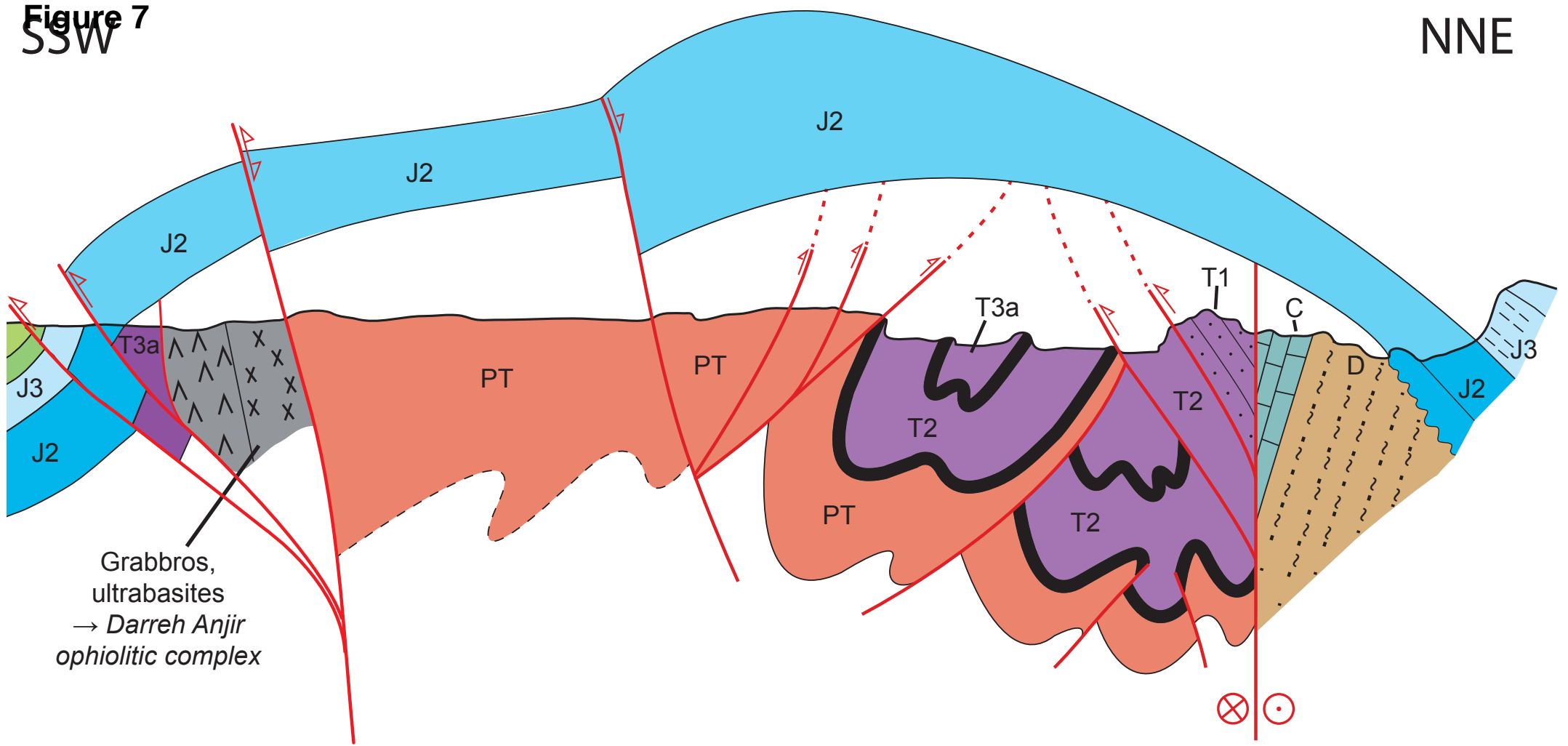


Figure 8

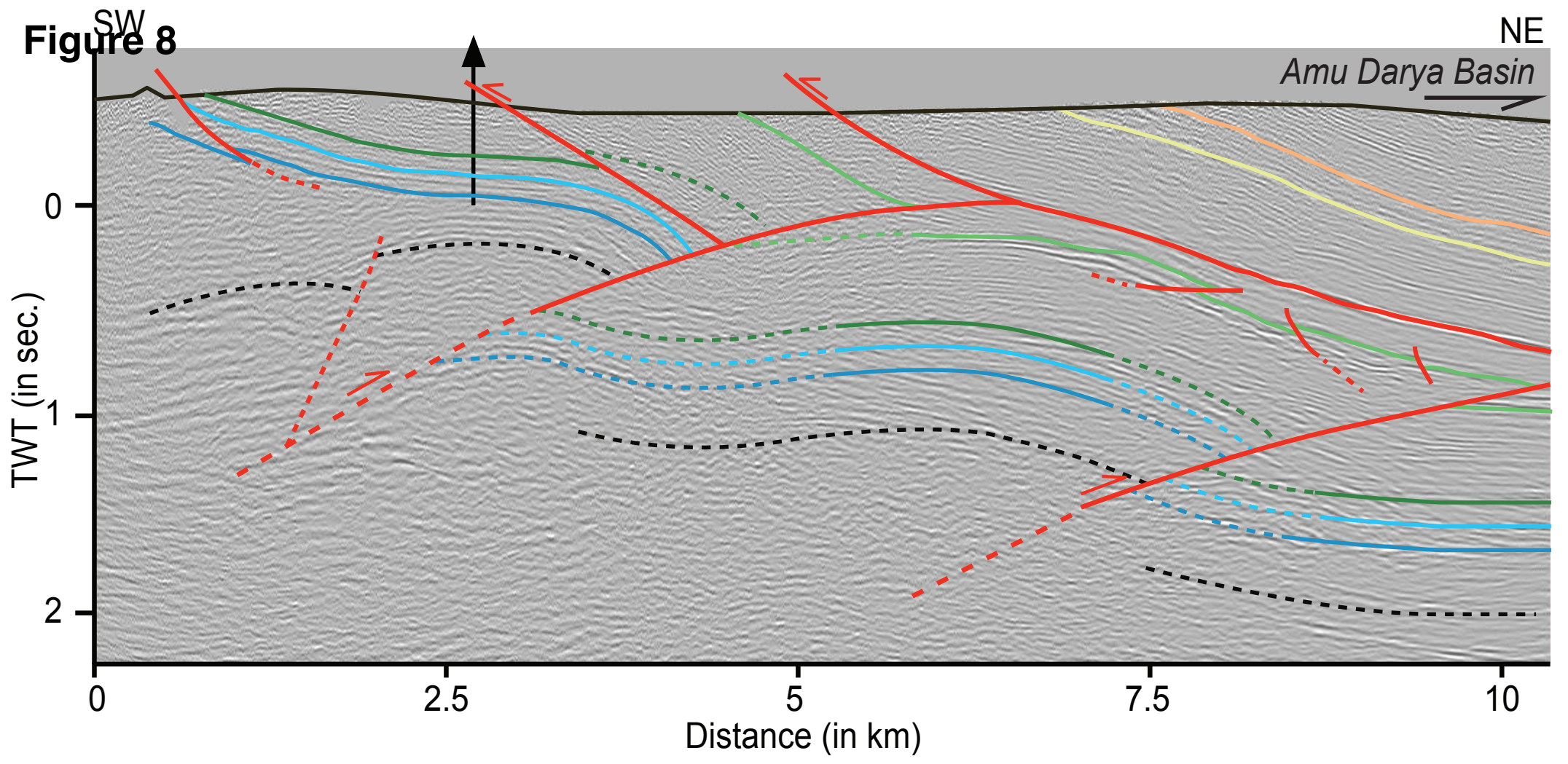
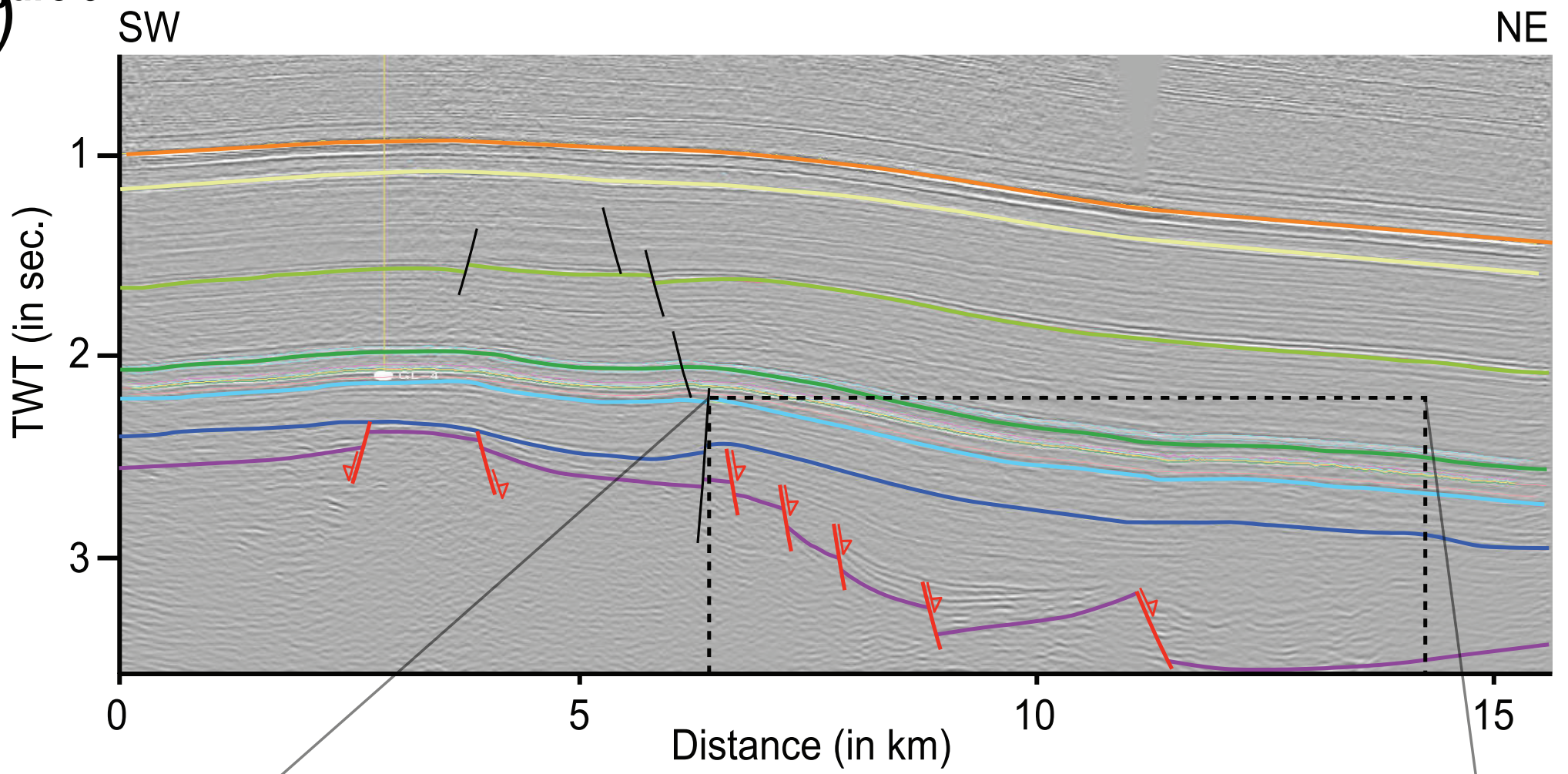




Figure 9  
a)



b)

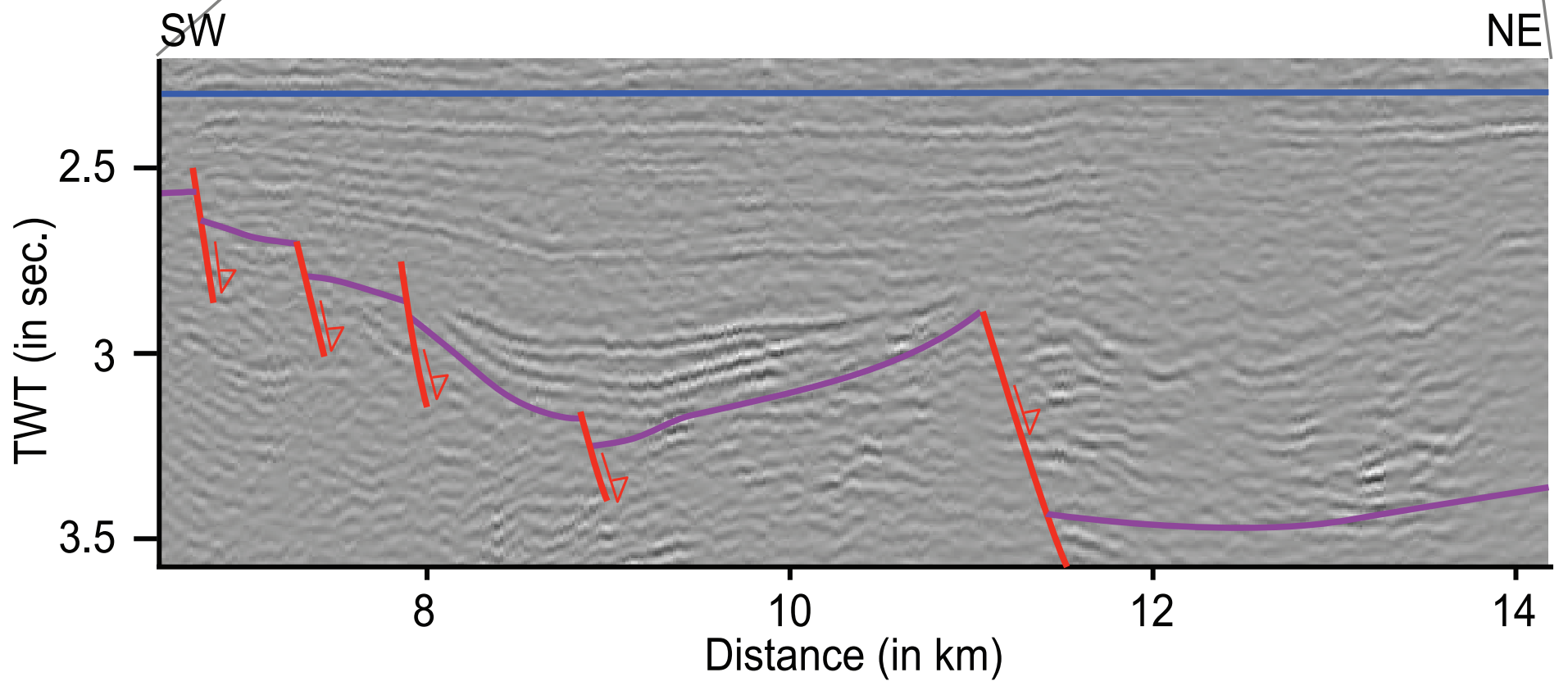




Figure 10

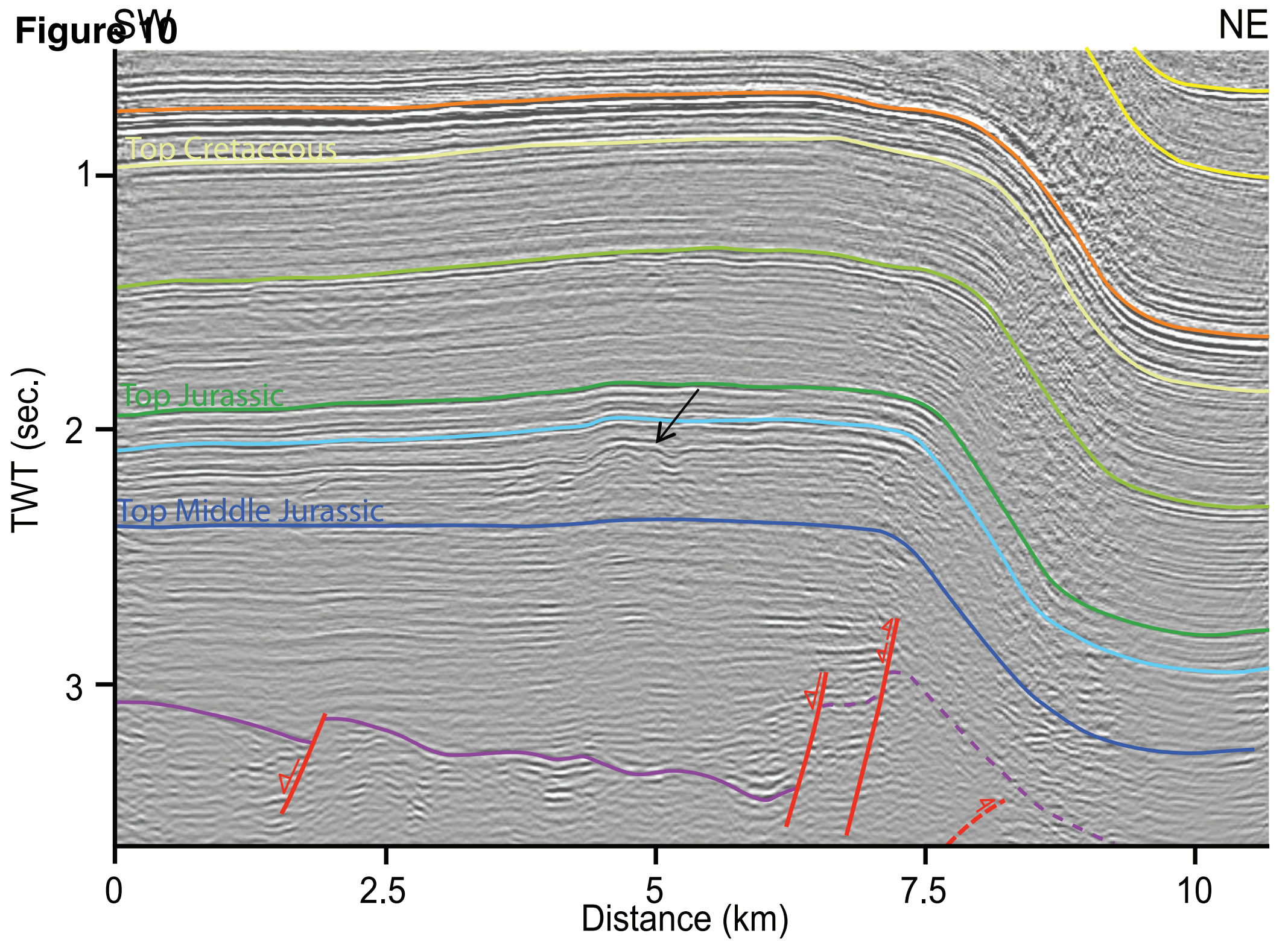


Figure 11

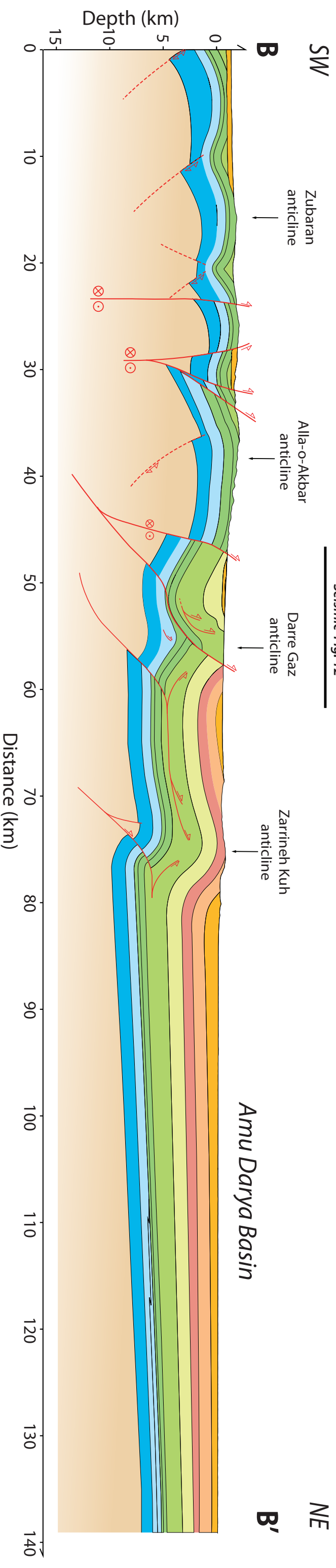




Figure 12

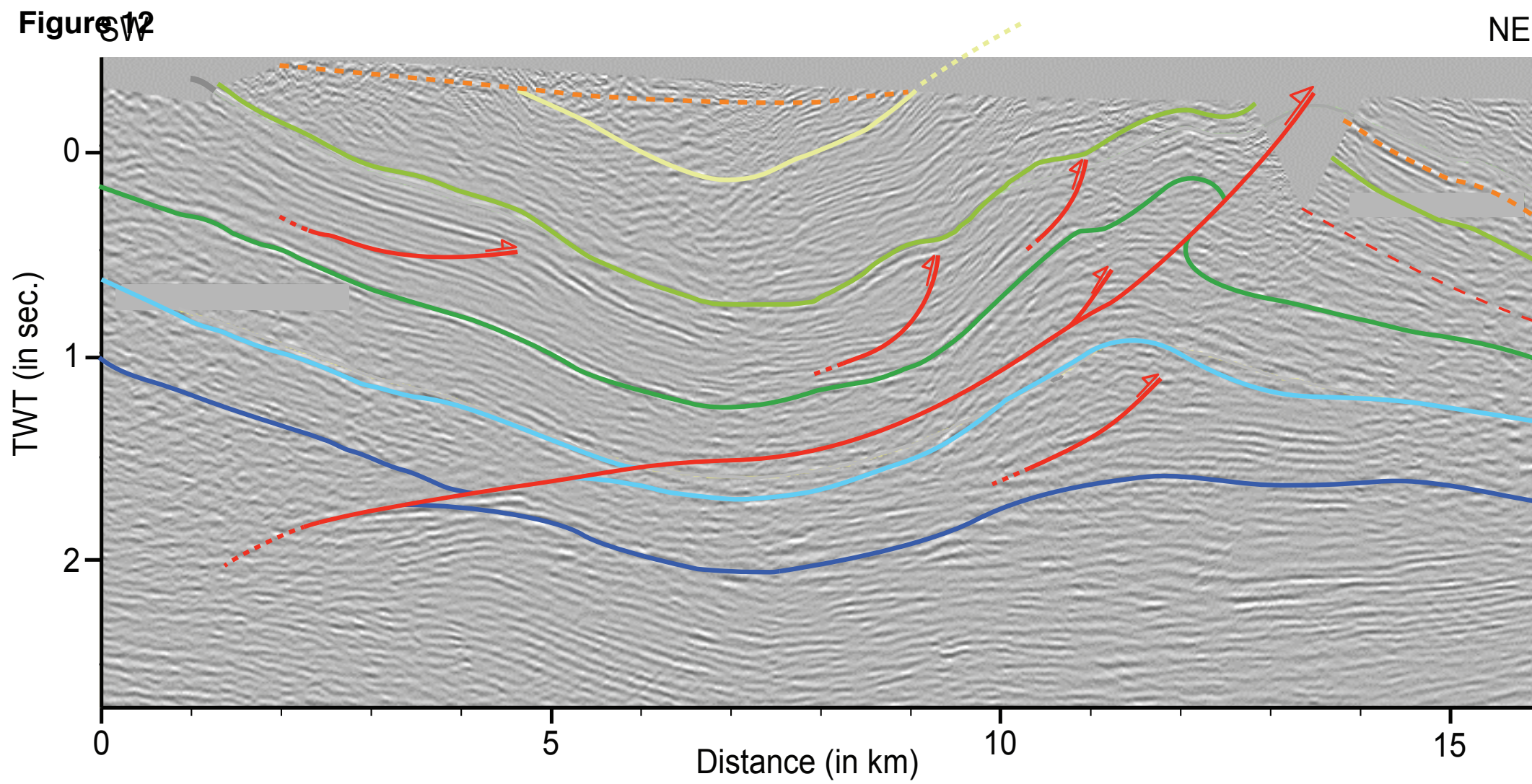


Figure 13

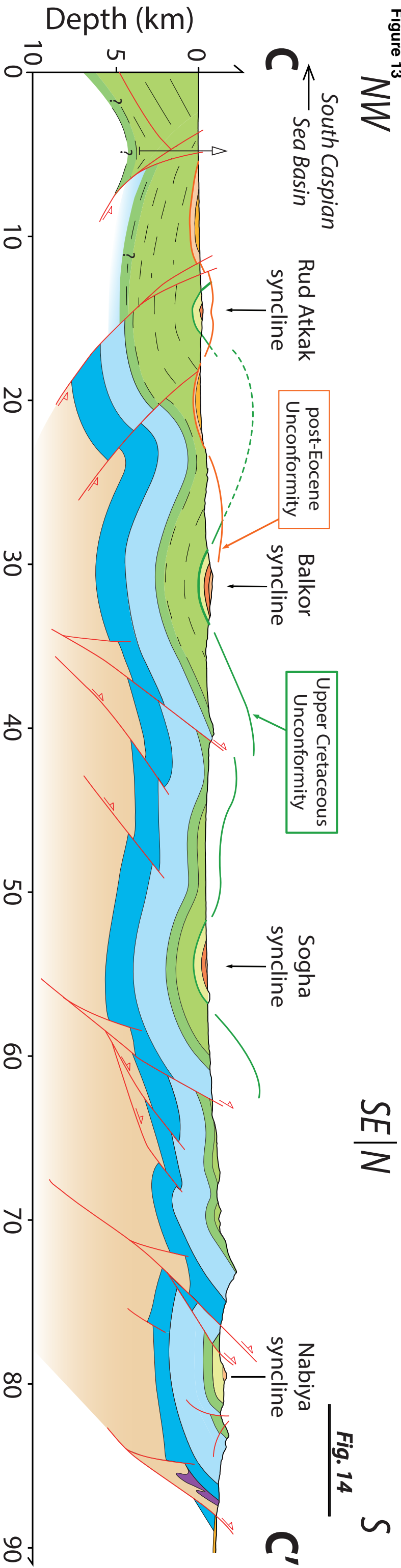
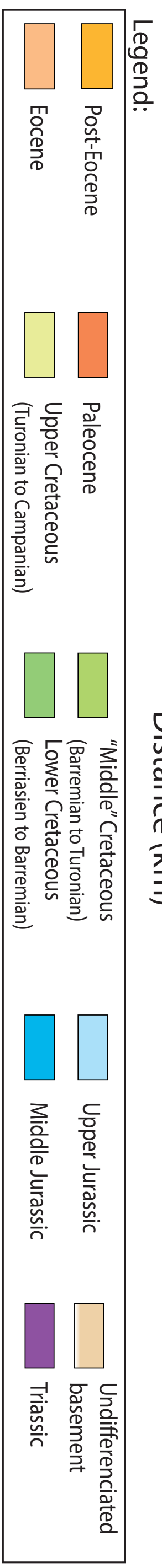


Fig. 14



**Figure 14**

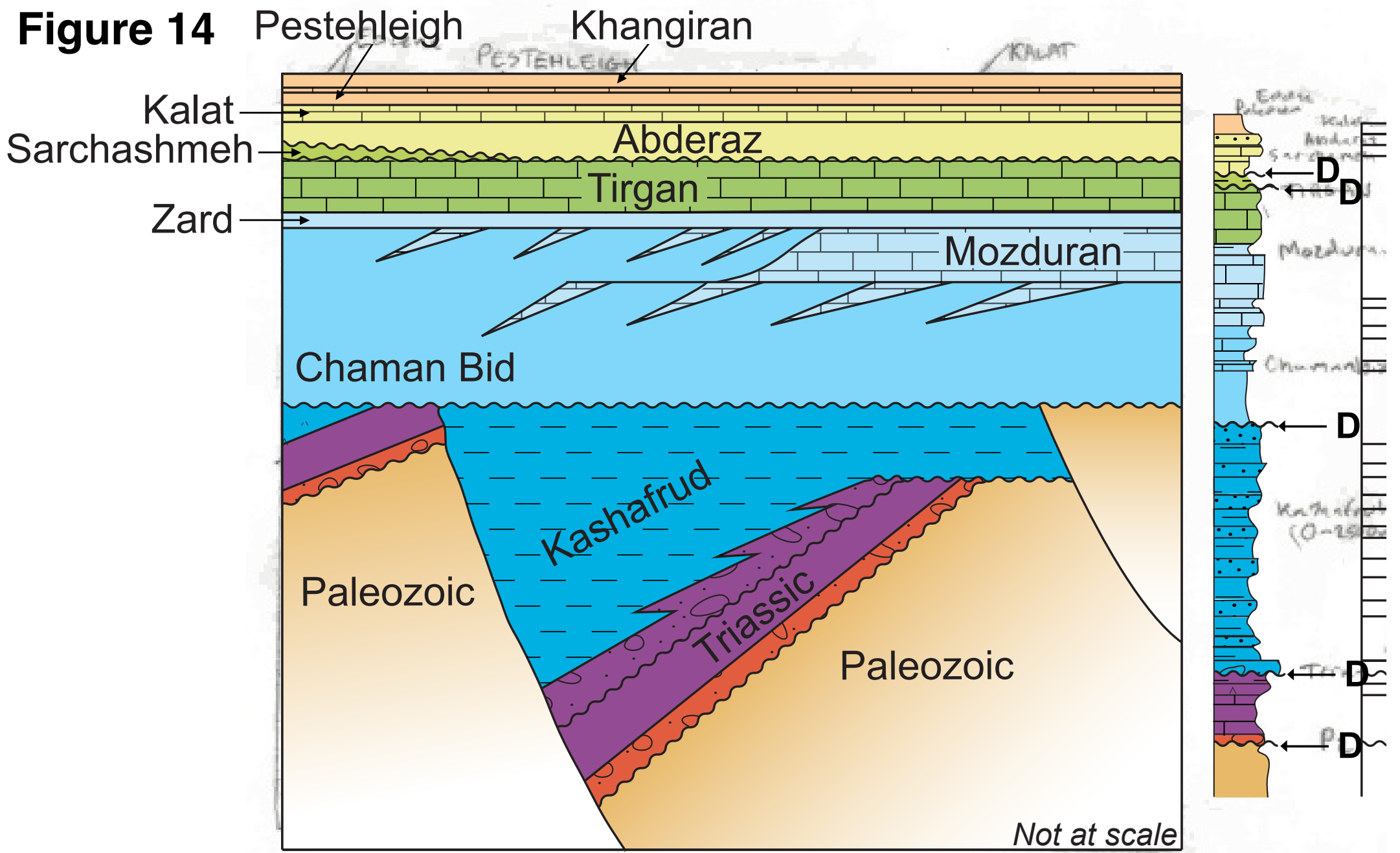
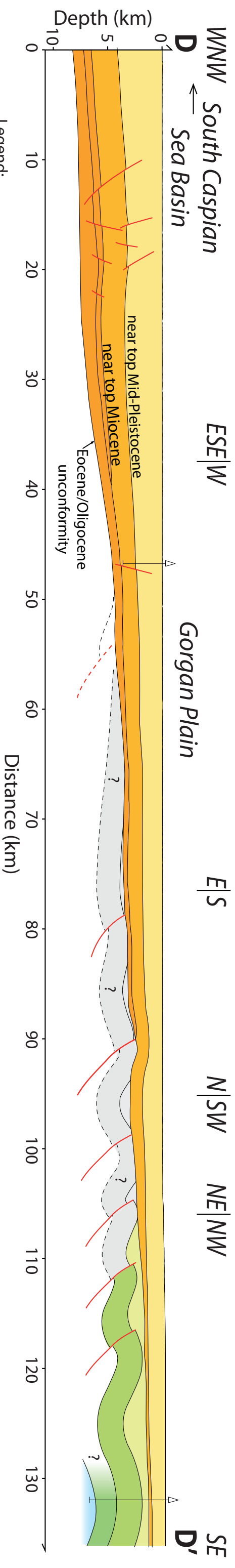


Figure 15

Seismic Fig. 17

Seismic Fig. 16

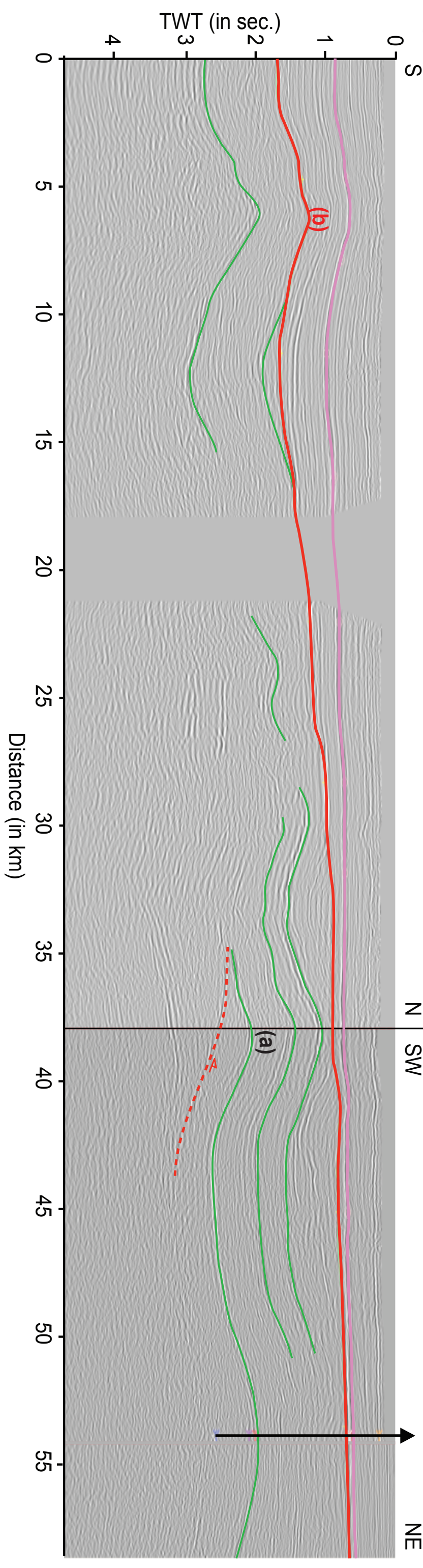


Legend:

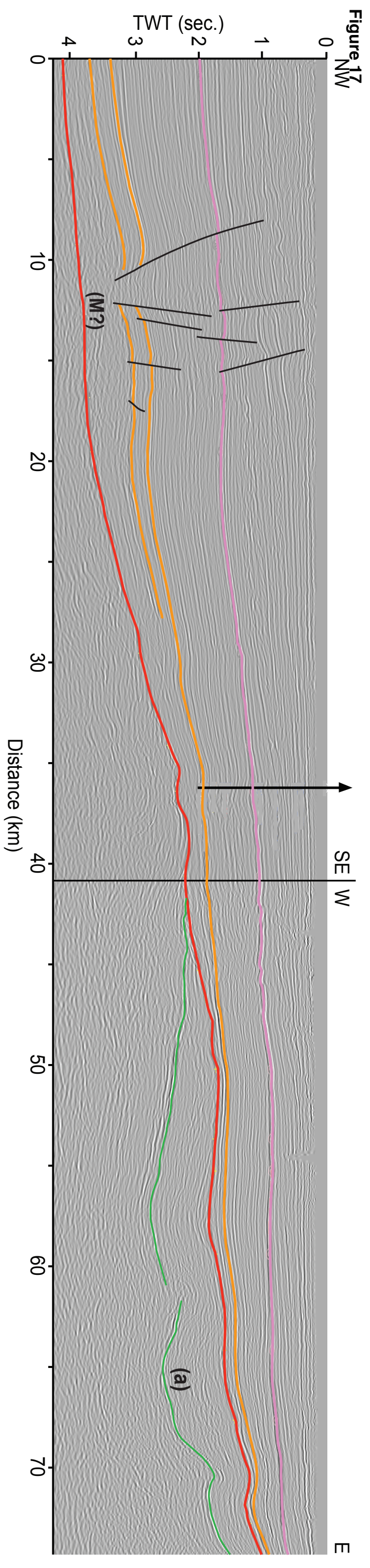
- Pleist.-Q.
- Mio-Pliocene
- Oligocene
- Upper Cretaceous (Turonian to Campanian)
- "Middle" Cretaceous (Barremian to Turonian)
- Lower Cretaceous (Berriasian to Barremian)
- Upper Jurassic
- Unknown age

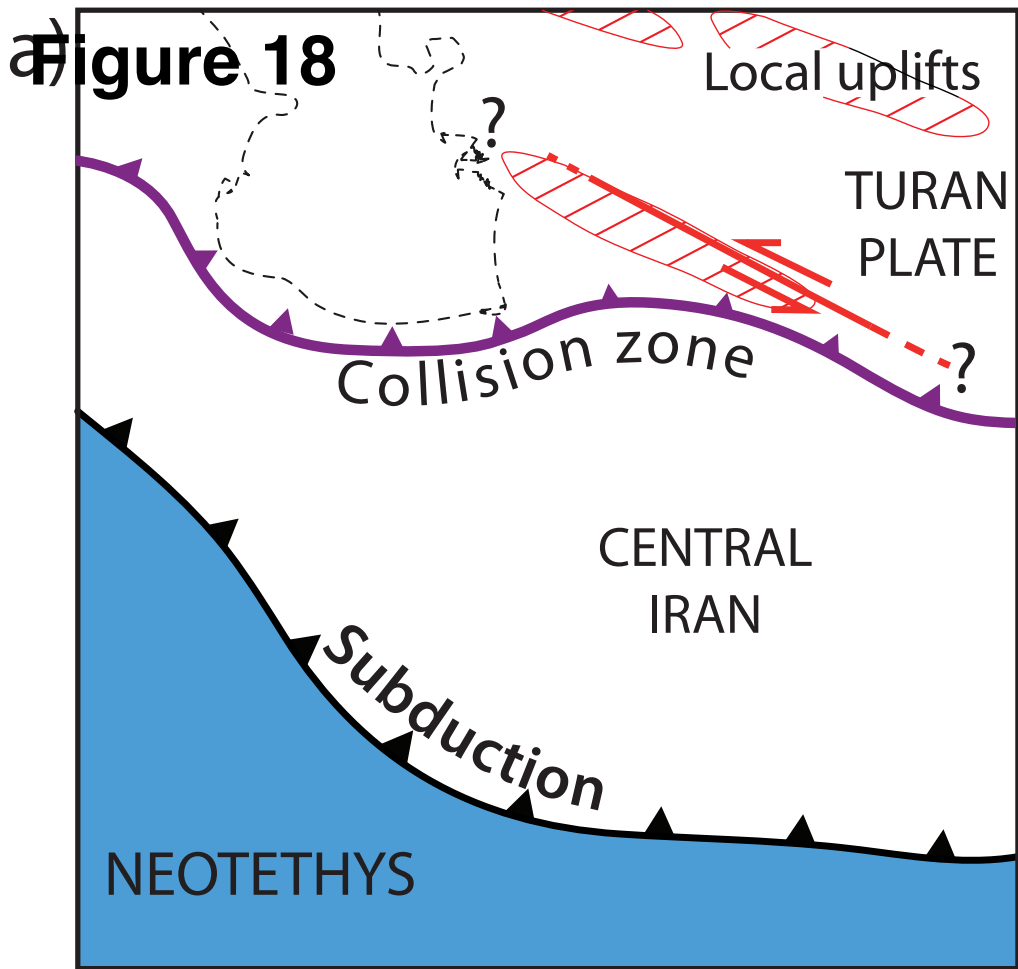


Figure 16

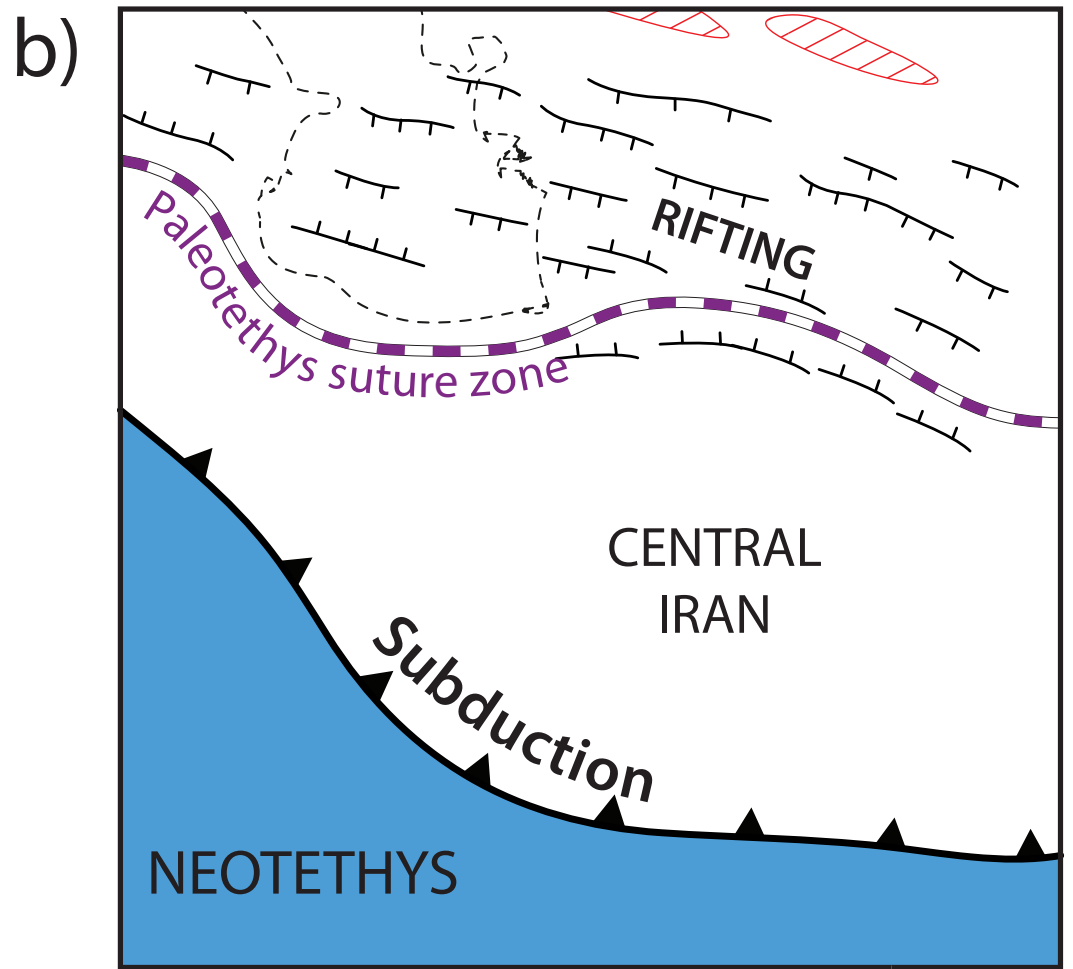




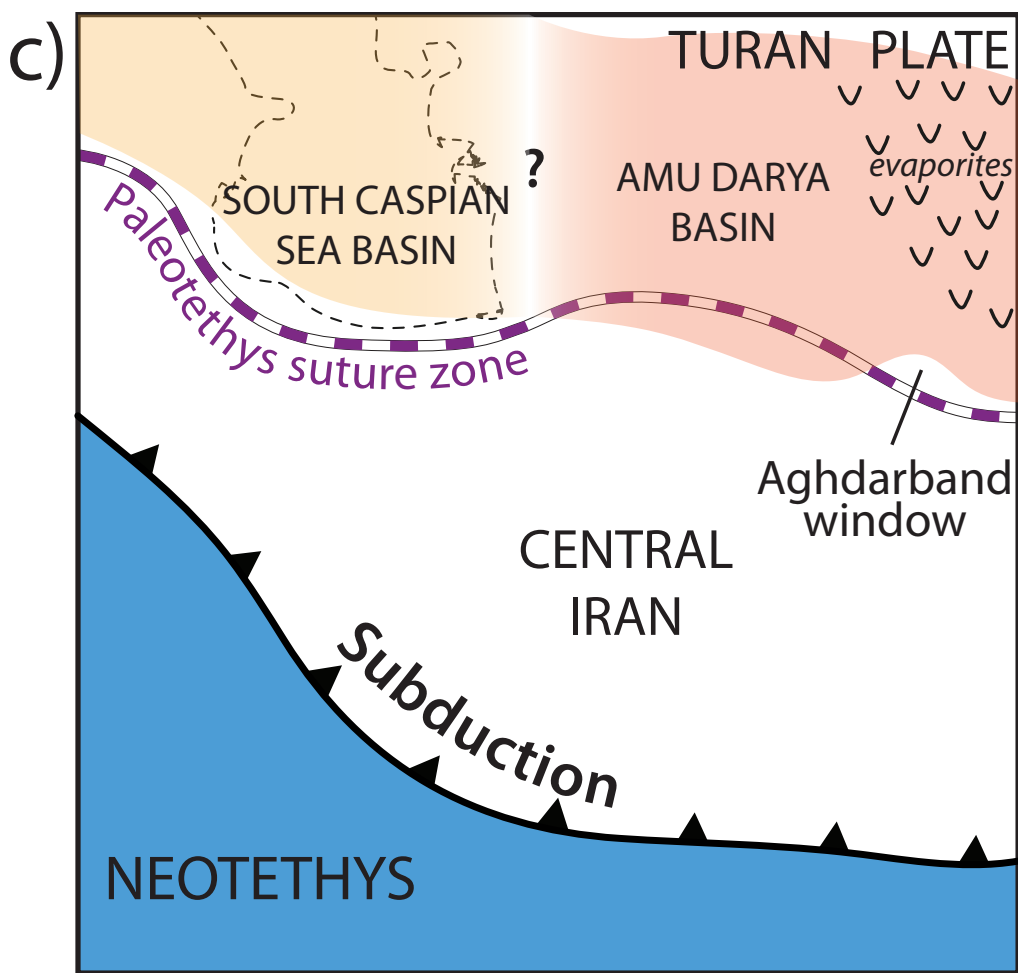




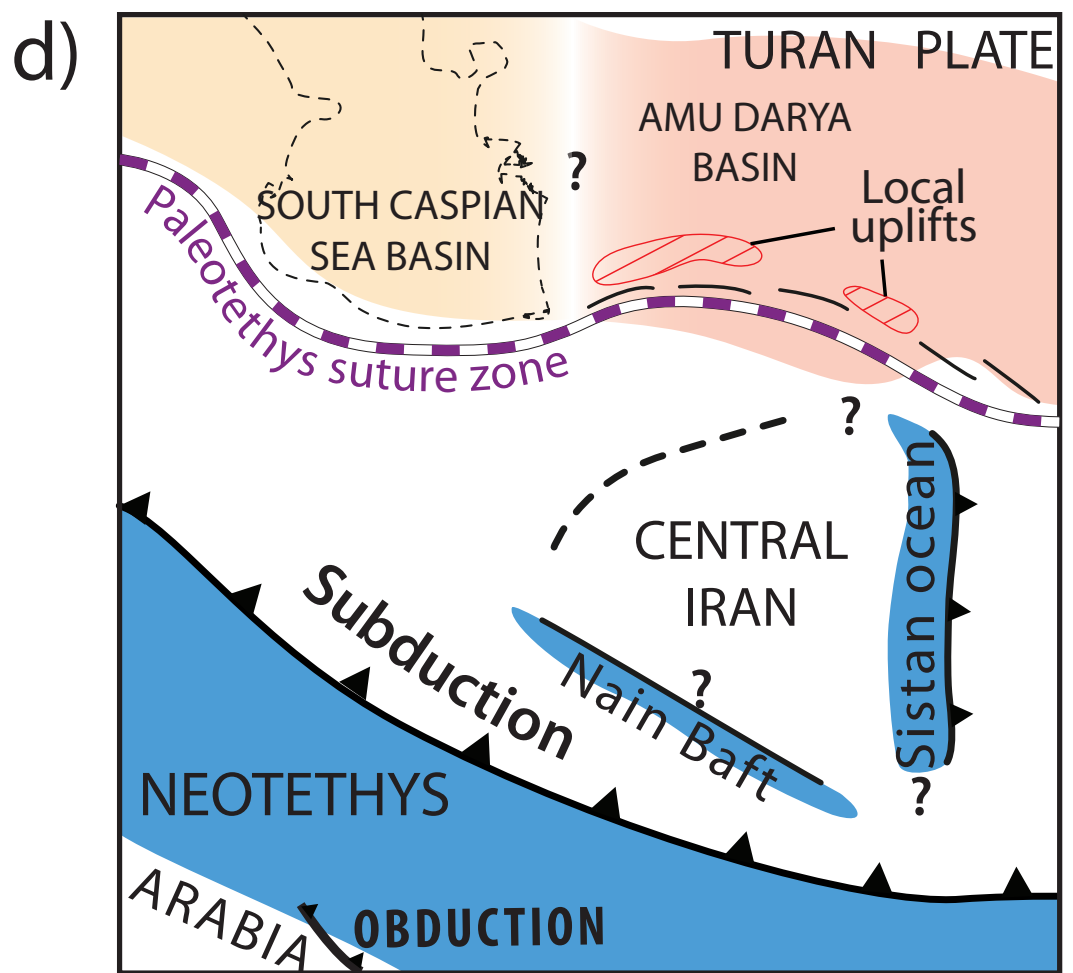
Late Triassic - Early Jurassic



Middle Jurassic

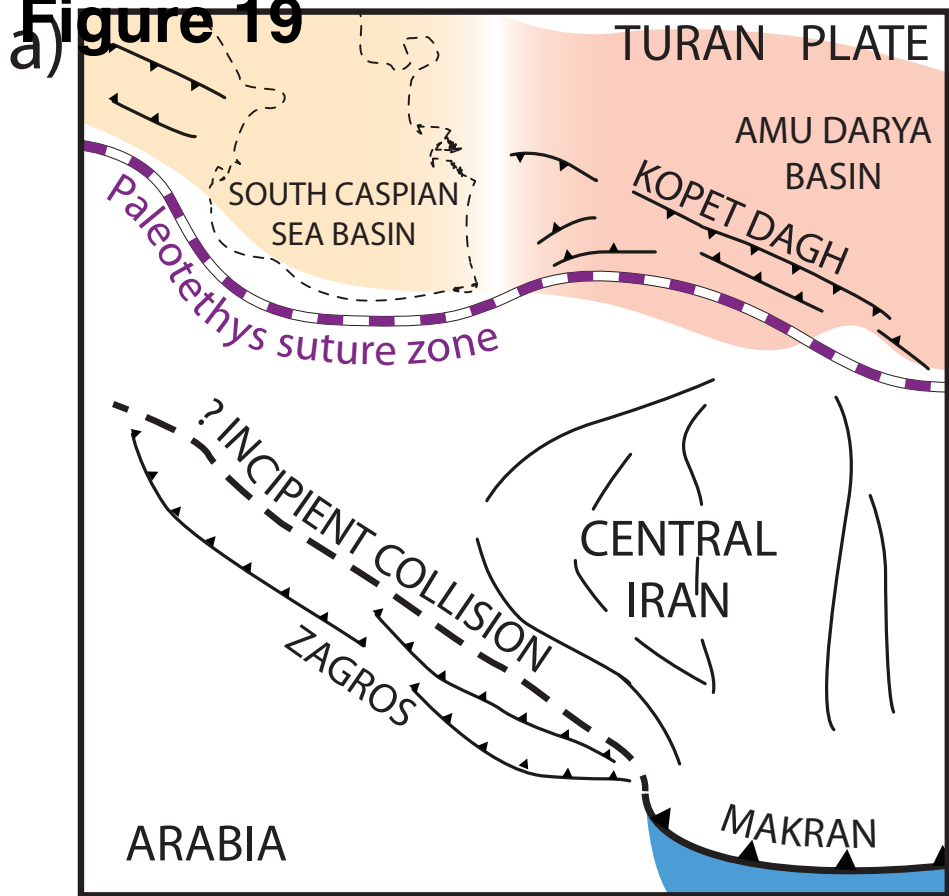


Latest Jurassic - Early Cretaceous

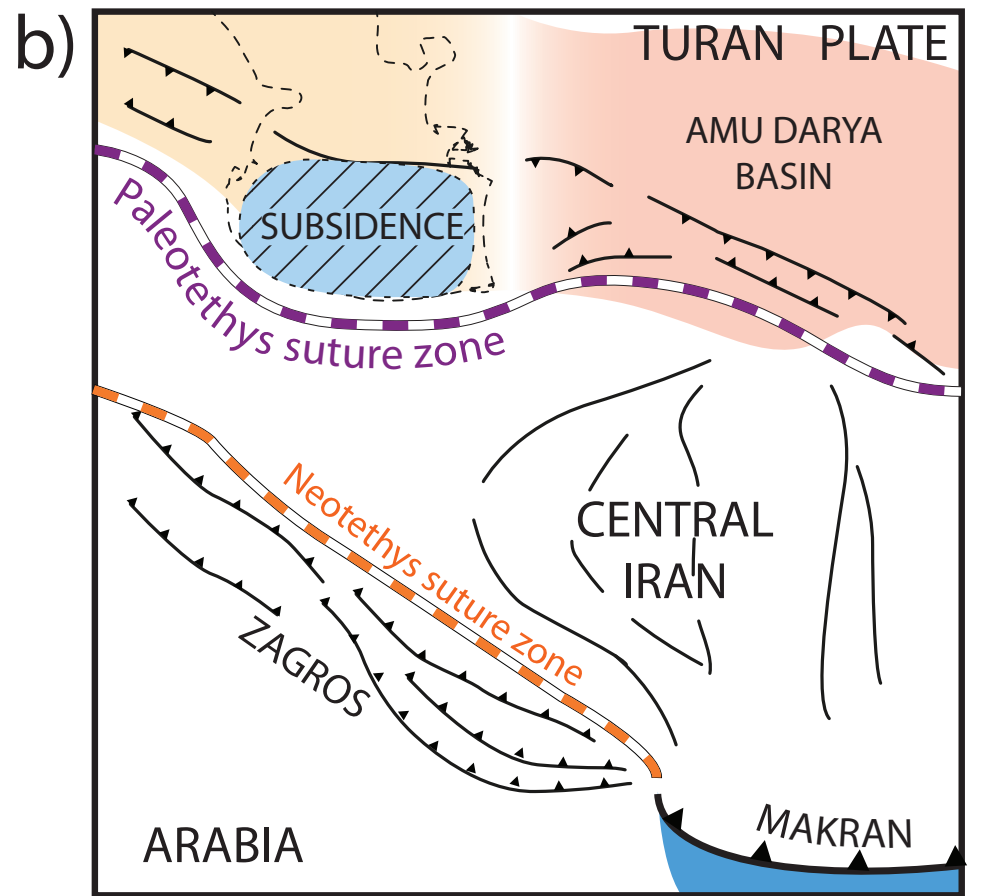


Late Cretaceous - Eocene

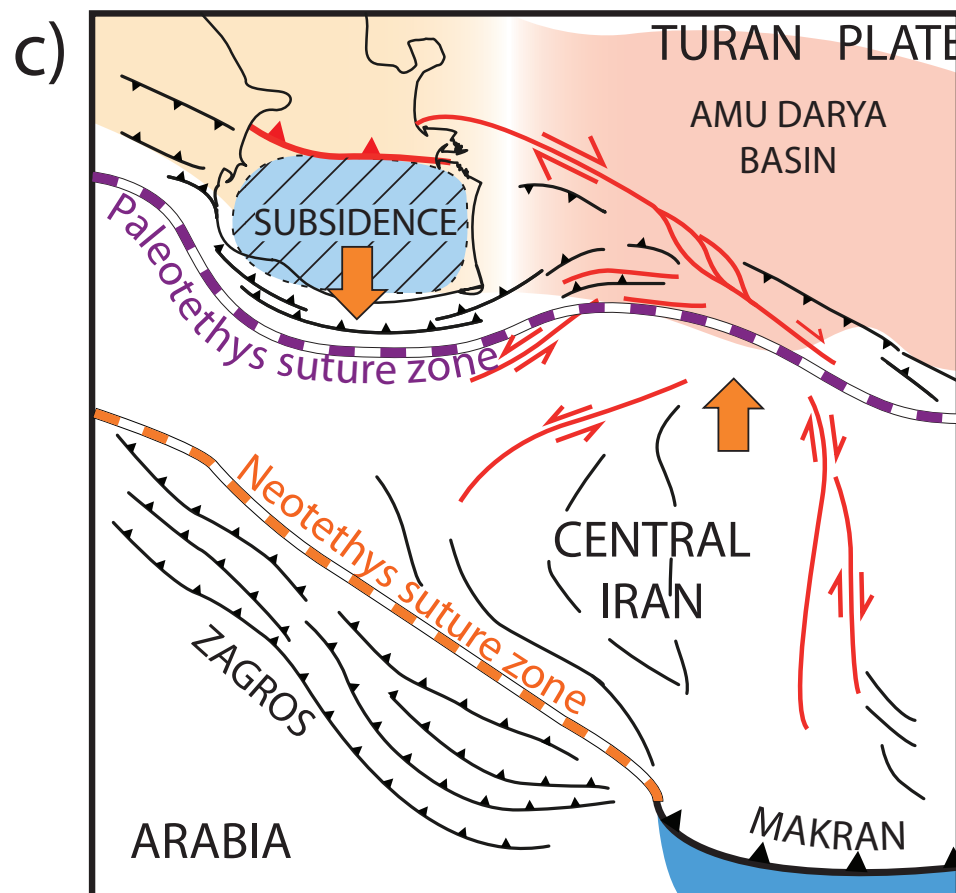
**Figure 19**



Late Eocene - Early Oligocene



Oligocene - Middle Pliocene



Late Pliocene - Present



Table 1

Era	Period	Epoch	Zone	fm	Sample reference	Sample location	Lithology	Observed Nannofossils		
Cenozoic	Paleogene	?Oligocene-Neogene conglomerates								
		Late Eocene	NP19	Khangiran	184AR 185AR 186AR	N37°29'29.2" E59°10'18.4" and N37°29'25.5" E59°09'90.6"	Marl with thin limestone beds			
					10-318 10-322 to 324 12-104 12-119 181AR - 182AR	N37°31'64.2" E59°09'35.6"	Marl with thin limestone and sandy beds	R. umbilica Ch. solitus D. tassi nodifus D. roemmilensis		
					10-145 10-146		Marl with thin limestone beds	Ch. gigas Ch. solitus N. alatus S. bifurcatoides		
					10-139 to 10-144		Marl with thin limestone beds	D. sublodoensis D. chiastolithus D. nonradiatus D. kuepperi		
		Lower Eocene	NP12		12-135 to 12-140 178AR	N37°31'64.2" E59°09'35.6"	Limestone with marl intercalated often dolomitized	D. lodoensis M. tribrachiatus S. radians T. pulcherima Ch. Solitus D. binodosus L. nascens		
		Upper Paleocene	NP9	Chehel-Kamar	10-103 10-104		White limestone and light marls	D. multiradiatus F. tympaniformis H. kleinpellii		
					10-111	N36°17'23.2" E66°35'29.4"		Ch. danicus F. tympaniformis		
		Lower Paleo.	NP2	Pestehleigh	10-108	N36°17'23.2" E66°35'29.4"	Continental red sandstone and siltstones - Some conglomerates with short marine	C. pelagicus B. sparsus Cr. Tenuis E. subpertusa		
		Upper Cretaceous	Upper Campanian	Maastrichtian : GAP						
				Kalat	10-41 10-43 to 45 11-253 to 257	N36°17'36.6" E60°33'21.6"	Massive limestone, limestone with rudists marls + lumachelles beds	Q. quadratugohicus Q. quadratrifidus B. borinsoniatarca E. eximius		
					Abtalkh	10-147 to 150 11-315 12-21 to 26	N36°26'07.9" E60°26'50.3" and N37°31'47.1" E57°47'39.0"	Marl	B. parca E. eximius R. anthophorus	
						Abderaz	10-29 11-200 to 205 12-37 12-93 to 96	N36°10'46.0" E60°33'46.0" N37°36'37.8" E58°45'36.0" N37°26'58.0" E56°56'45.0"	Limestone with chert nodules and marl. Flat channels	Q. gothicum Q. trifidum

Era	Period	Epoch	Zone	fm	Sample reference	Sample location	Lithology	Observed Nannofossils		
Mesozoic	Upper Cretaceous	Lower Campanian		Abderaz	10-26 to 28 63, 10-151, 11-251, 11-252, 12-17	N28°08'17.0" E40°63'15.0" and N36°26'52.5" E60°26'46.7"	Limestone with chert nodules and marl. Flat channels	E. eximius B. parca R. anthophorus		
					10-20 to 25 11-250, 12-34, 12-120	N37°36'23.8" E58°45'32.0" and N37°41'28.5" E56°06'46.8"	Limestone with chert nodules and marl. Flat channels.	M. purcatus R. anthophorus E. eximius		
	<b>Turonian, Coniacien and L. Santonian : HIATUS</b>									
	Lower Cretaceous	Cenomanian			AiTamir	10-13 to 19 11-351 to 361, 11-369 to 373, 11-376, 11-377, 12-65 to 67	N37°56'49.6" E56°55'36.2"  N38°00'37.6" E57°00'25.0"  N37°58'48.9" E47°18'47.4"	grainstone, sandstone siltstone or dark, brownish siltstone claystone	Barren of nannofossils with flute channels and wood on the base	
						11-246 to 248 12-148 à 150	N37°56'56.7" E55°39'40.1"	fine grained sandstones, marl, dark sandstone, claystone with concretions	E. turriseiffelii P. cretacea P. albianus N. fragilis	
		<b>Gap of barren of nannofossils</b>								
		Aptian (upper)				Sachermeh	10-9, 10-96 to 98 11-244 to 245, 11-303 to 305, 11-349		"pencil marls"  siltstone, marl with lumachelles, beds of thin limestone, beds orbitoids	E. floralis R. angustus N. wasseli N. quadriangulus N. carniolensis latus
							10-2 to 7, 11-297 to 29, 11-344 to 348 11-362 to 365	N37°53'17.3" E50°55'57.8"		N. colomii N. circularis N. steinmossii G. margerellii
		Barremian				Tirgan	10-84 to 90, 11-241 to 243	N36°00'40.2" E60°55'32.6"	massive limestones rich in orbitoid marl intercalations	
	<b>Valanginian- Hauterivian: Gap or not yet determined</b>									
	Upper Jur.	Oxf. Kim. Tith			Mozduran			recifal limestones bedded limestones with marl sandstones with conglomerates in chorrels	<i>low diversified assemblages no precise age determination</i>	
						Berriasian		Surijeh	11-325 to 328	
	Mid. Jur.	Callovian		Chaman Bid	11-216 to 222				N47°46'69.3" E41°37'85.8"	siltstone marl



